Citing this contribution:
N. Tessler, http://www.ee.technion.ac.il/orgelect/Useful_Information.htm, 2009.

Experimental techniques to determine transport parameters

Table of Contents

I. The basic framework

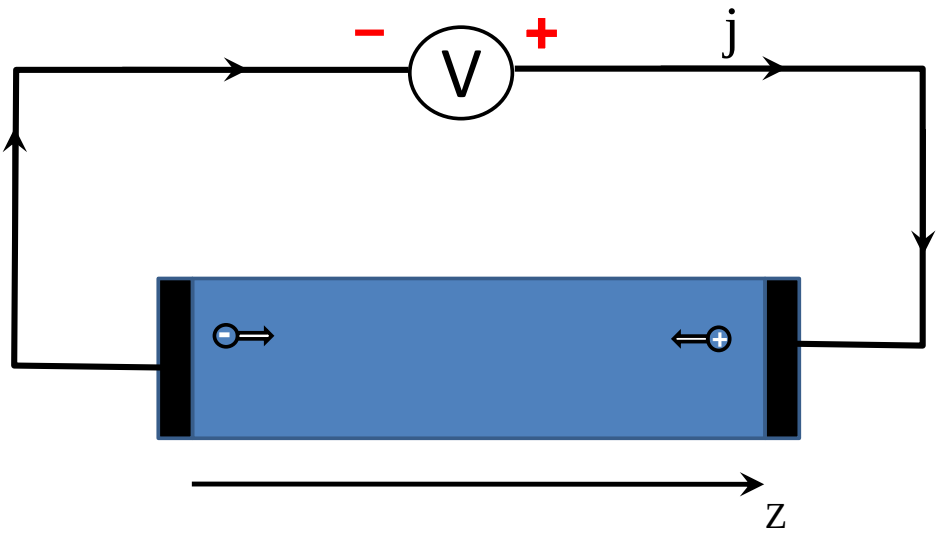

Figure 1. The convention used in this document for describing the various device parameters.

$$(1)\ \frac{\partial}{\partial t}n_e(z,t)=\frac{\partial}{\partial z}\left[D_e\frac{\partial}{\partial z}n_e(z,t)+\mu_e(E)n_e(z,t)E(z,t)\right]-R(z,t)+G(z,t)$$

$$(2)\ \frac{\partial}{\partial t}n_h(z,t)=\frac{\partial}{\partial z}\left[D_h\frac{\partial}{\partial z}n_h(z,t)-\mu_h(E)n_h(z,t)E(z,t)\right]-R(z,t)+G(z,t)$$

$$(3)\ \frac{d}{dz}E=\frac{q}{\varepsilon\varepsilon_0}\left(n_h(z)-n_e(z)-n_{h0}(z)+n_{e0}(z)\right)$$

$$(4)\ V(t)=-\int_0^d E(z,t)dz$$

$$(5)\ \frac{\partial}{\partial t}S(z,t)=FR(z,t)+\frac{\partial}{\partial z}\left[D_s\frac{\partial}{\partial z}S(z,t)\right]-\frac{S}{\tau}$$

As in the convention shown in Figure 1 positive current flows in the –z direction (right to left) we added a minus sign to the conventional equations:

$$(6)\ \begin{cases} j_e(z,t) = q\mu_e n_e(z,t)E(z,t) + qD_e \dfrac{d}{dz} n_e(z,t) \\ j_h(z,t) = q\mu_h n_h(z,t)E(z,t) - qD_h \dfrac{d}{dz} n_h(z,t) \end{cases}$$

$$(7)\ -j(z,t) = \varepsilon\varepsilon_0 \frac{d}{dt} E(z,t) + j_e(z,t) + j_h(z,t)$$

$$(8)\ \frac{d}{dz} j(z,t) = 0$$

Here n_e, n_h, and S are the electron, hole, and singlet exciton density, respectively. D_e and D_h are the electron and hole diffusion coefficients. In most cases we'll assume that the Einstein diffusion relation holds for these systems hence, $D_e = \mu_e kT/q$ and $D_h = \mu_h kT/q$ (where q is the unit of electrical charge). z is the distance from the cathode and ε is the permeability (taken to be ε=3).

In the following sections we will use numerical simulation which solves the above equations self consistently to provide some insight and hopefully a bit intuition too.

II. J-V

The simplest method to extract mobility is to insert the material in between two electrodes and measure the current-voltage characteristics. The only catch is that in order to be able to extract parameters from the device we need to know the physical mechanism governing the J-V curves and in organic device this is often not trivial. For example:

The general expression for SCL current is

(9) $V = \sqrt{\frac{8J}{9\varepsilon\varepsilon_0\mu}}\left\{\left(d+K\right)^{3/2} - K^{3/2}\right\}$

where K is given by $K = \frac{J_{SCL}\varepsilon\varepsilon_0}{2N_0^2e^2\mu}$ with N_0 being the injected charge density at the contact.

If the contact is not limiting (N_0 is large and K is small compared to d):

(10) $J = \frac{9}{8}\varepsilon\varepsilon_0\mu\frac{V^2}{d^3}$

If the contact is limiting (N_0 is small and K is large compared to d):

(11) $J = qN_0\mu\frac{V}{d}$

Equations (10) and (11) are describing the same material but for different contact properties. Moreover, if the contact material is metallic and the contact barrier lowering due to image force has to be accounted for than equation (11) becomes a bit more complicated as the effective N_0 may be a function of the applied bias.

For more details on how to analyze J-V curves see [1, 2]

III. Time of flight

The time of flight (TOF) is a method used to measure the time it takes electrons to travel across a sample, i.e. between the excitation and detection points.[3, 4] The standard time of flight is:

Figure 2. Typical experimental set up of the time of flight (TOF) technique.

To create some basic intuition for the TOF method we present in Figure 3 results of a numerical simulation of a 1μm long device which is biased at 20V using non-injecting contacts. The device is excited using light pulse assuming ~20nm absorption depth. The different pictures show that very quickly the charge packet assumes the shape of a Gaussian which broadens as it propagates (the span of the x-axis is kept at 350nm for better visualization of the effect). We also note that the current starts to drop as the packet starts to exit the device.

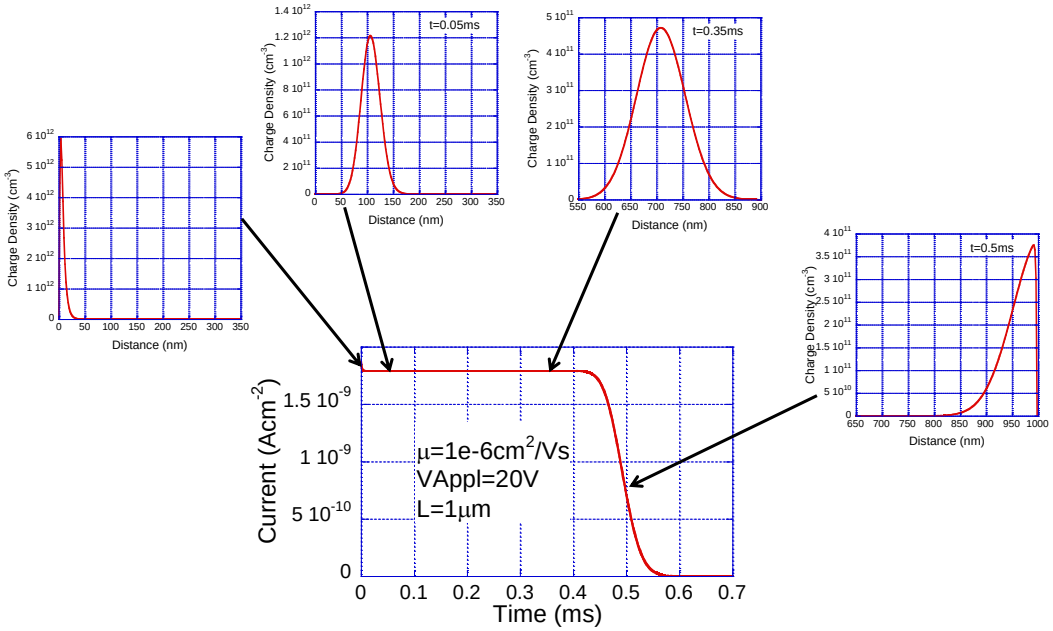

Figure 3. Simulated current response to a pulse excitation generating charges very close to the (non-injecting) contact. The surrounding figures show snap shots of the charge density distribution at the marked points in time.

The parameter set used in the simulation is:

Parameter	**Value**
Length	d=1000nm
Bias	V=20V
Absorption length	L_{abs}=20nm
Cathode	$n_e(0,t)=10^{10}cm^{-3}$ $n_h(0,t)=10^{10}cm^{-3}$
Anode	$n_e(d,t)=10^{10}cm^{-3}$ $n_h(d,t)=10^{10}cm^{-3}$
Electron mobility	$\mu_e=10^{-6}cm^2/Vs$
Hole mobility	$\mu_h=10^{-6}cm^2/Vs$
Total density of states	$10^{21}cm^{-3}$

To formally analyze this experiment we rewrite equations (1)

$$(12)\ \frac{\partial}{\partial t}n_e(z,t)=\frac{\partial}{\partial z}\left[D_e\frac{\partial}{\partial z}n_e(z,t)+\mu_e(E)n_e(z,t)E(z,t)\right]-R(z,t)+G(z,t)$$

Assuming that for t>0 one can neglect generation and recombination and that we are dealing only with one type of carriers (electrons), equation (7) is written as:

$$(13)\ -j(z,t)=\varepsilon\varepsilon_0\frac{d}{dt}E(z,t)+q\mu_e n_e(z,t)E(z,t)+qD_e\frac{d}{dz}n_e(z,t)$$

Assuming D and μ to be independent of position (and charge density) and that the charge density is too low to significantly alter the electric field[1] we rewrite (12):

$$(14)\ \frac{\partial}{\partial t}n_e(z,t)=D_e\frac{\partial^2}{\partial z^2}n_e(z,t)+\mu_e(E)E(z,t)\frac{\partial}{\partial z}n_e(z,t)$$

Neglecting the transient phenomena close to t=0, the steady state solution to the above is:

$$(15)\ n_e(z,t)=\frac{n_{e0}}{2\sqrt{\pi D_e t}}e^{-\frac{\left(z-\mu_e\frac{V}{d}t\right)^2}{4D_e t}}$$

Namely, shortly after the pulse excitation the charge packet will assume the shape of a Gaussian (see Figure 3). Integrating equation (13):

[1] In cases where the sample is doped we require that the sum of the injected and dopant (n_{e0}) induced charges is small enough.

$$(16)\quad -j(t)=\frac{1}{d}\int_0^d -j(z,t)dz=\frac{1}{d}\int_0^d q\mu_e E n_e(z,t)dz=-\frac{1}{d}q\mu_e\frac{V}{d}\int_0^d \frac{n_{e0}}{2\sqrt{\pi D_e t}}e^{-\frac{\left(z-\mu_e\frac{V}{d}t\right)^2}{4D_e t}}dz$$

Performing change of variables:

$$(17)\quad -j(t)=-\frac{1}{d}q\mu_e\frac{V}{d}\int_{\frac{-\mu_e\frac{V}{d}t}{2\sqrt{D_e t}}}^{\frac{d-\mu_e\frac{V}{d}t}{2\sqrt{D_e t}}}\frac{n_{e0}}{\sqrt{\pi}}e^{-z^2}dz$$

Using $\int_0^a e^{-z^2}dz=\frac{1}{2}\sqrt{\pi}\cdot erf(a)$ and assuming $\frac{-\mu_e\frac{V}{d}t}{2\sqrt{D_e t}}$ is negatively large enough to be considered $-\infty$:

$$(18)\quad j(t)\simeq\frac{n_{e0}}{d^2}q\mu_e V\cdot\left\{\frac{1}{2}+\frac{1}{2}erf\left(\frac{d-\mu_e\frac{V}{d}t}{2\sqrt{D_e t}}\right)\right\}$$

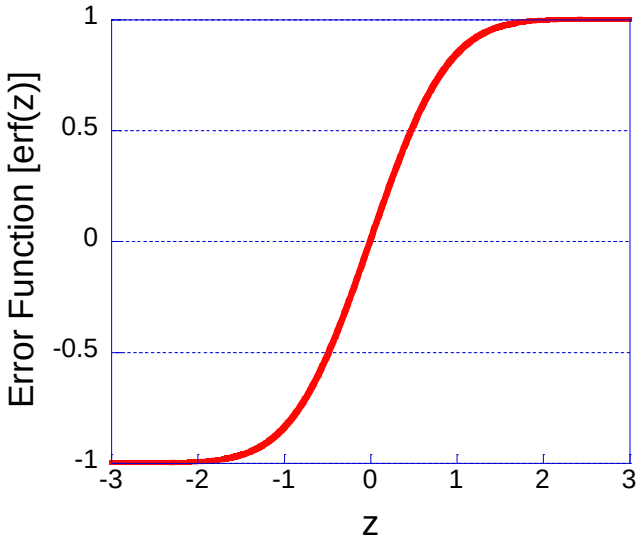

Figure 4. Graphic description of the error function (erf).

Examining equation (18) and Figure 4 we see that we have arrived at the functional form that is described by the numerical simulation shown in Figure 3. Equation (18) also shows that for the mobility extraction the transit time (τ_{tr}) is the point where the current

drops to half of its initial value (ignoring any transient phenomena close to t=0):

$$\tau_{tr} = t\big|_{j(t)=\frac{1}{2}j(0)} = \frac{d^2}{\mu_e V}$$

III.A. Charge injection layer

In cases where the sample is too thin or that the absorption length is too long it is common to employ a charge generation layer that selectively absorbs the excitation and supply the charges for the TOF measurement (see schematic at the top of Figure 5). For this technique to work properly one has to make sure that there is no barrier for transport from the charge generation layer to the bulk of the sample. If such a barrier exists it would alter the response in a manner demonstrated through the simulation presented in Figure 5 where the effect of the barrier is entered as $\exp\left(-\frac{\Delta E}{kT}\right)$.

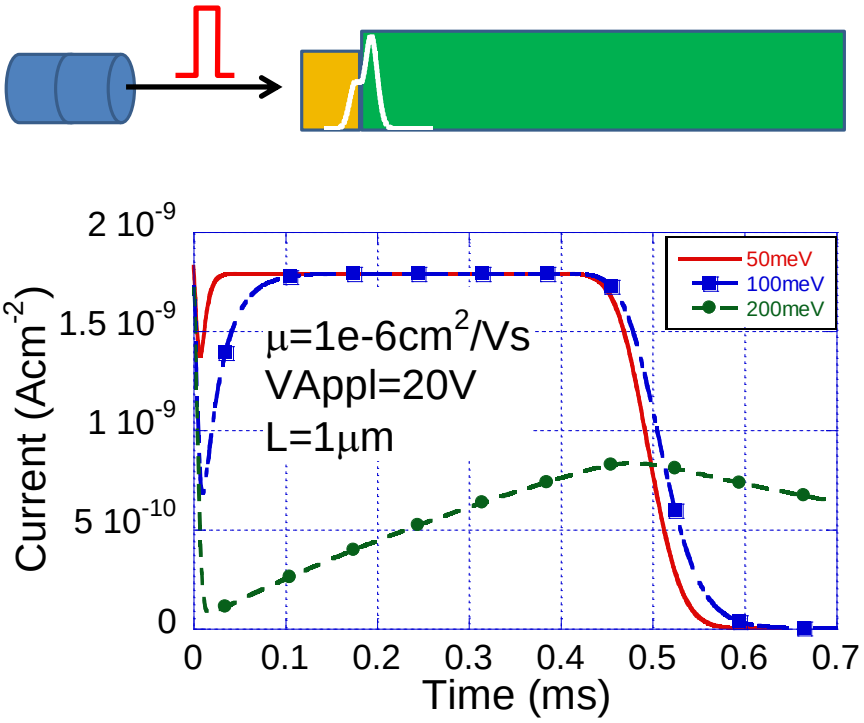

Figure 5. Simulated current response to a pulse excitation of the charge generation layer. The figure illustrates the effect of energy level mismatch which turns the charge generation layer into an effective charge trap the depth of which is dictated by the energy mismatch or barrier.

III.B. Dispersive mobility

The terms "Dispersive Transport" or "Dispersive Mobility" are typically used to describe a situation where the velocity of the carriers varies as a function of time and in some cases can be interpreted as if the carriers mobility is a function of time (typically a reducing function)[4-6]. As long as the velocity is changing by less than ~50% it may

still make sense to define an effective mobility to be the average velocity divided by the electric field. However, if the variation is large there is clearly no justification to relate the average velocity with a mobility value. The reasoning is that using this average "mobility" within the set of equations (1) to (8) will not allow us to even remotely reproduce the dynamics of the real system.

To illustrate what a dispersive curve would look like we repeated the simulation shown in Figure 3 and artificially set the mobility to be time dependent $\mu_e = 10^{-6}\exp(-t/\tau)$ with a time constant of τ=1.5ms.

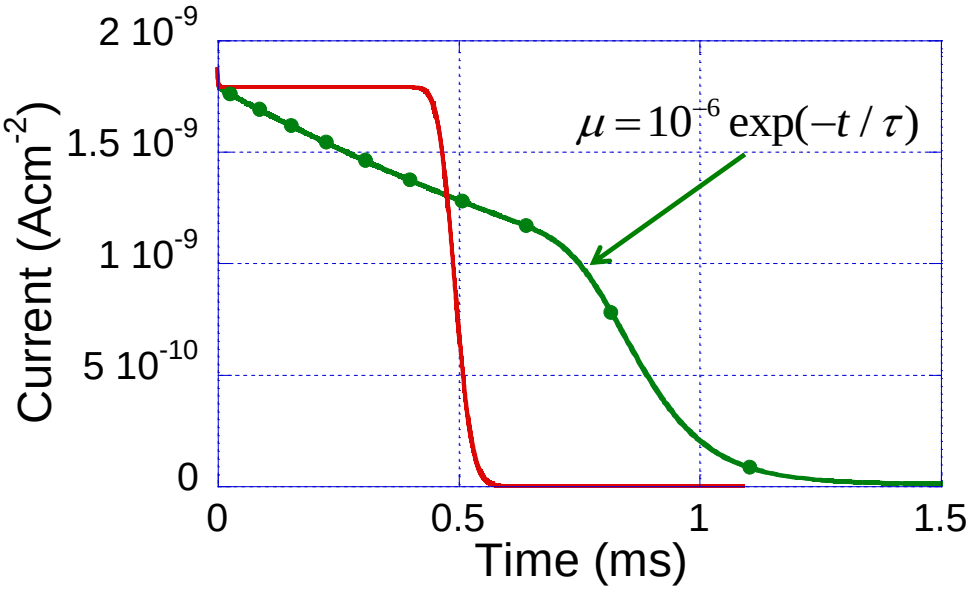

Figure 6. TOF transients for time independent mobility (full line, no symbols) and for a mobility decaying exponentially with time (τ=1.5ms).

IV. CELIV

As described in the previous section, the time of flight (TOF) is a basic method for evaluation of the charge carrier drift mobility in low mobility materials like organic semiconductors and amorphous hydrogenated silicon (*a*-Si:H). For the TOF method to be valid it is essential that the electric field experienced by the charge carriers is equal to the one being applied to the sample. If the material is slightly doped such that the free charge density (n_0) is relatively high than the redistribution of these charges and the creation of a depletion zone will alter the electric field distribution in the device. To ensure that the change of the electric field due to the depletion zone is negligible the free charge concentration has to be low such that $qn_0 d \ll \frac{\varepsilon\varepsilon_0}{d}V$. The left side denotes the maximum depleted charge that can be generated throughout the device and the right side is the charge density that can be accumulated at the facets of an ideal capacitor having the same dielectric constant (we note that in the context of doping, n_0 denotes the activated dopant density $n_0=n_{e0}$). This condition can also be expressed as requiring that the material dielectric relaxation time (τ_σ) is larger than the transit time (t_{tr}), i.e. $\tau_\sigma = \frac{\varepsilon\varepsilon_0}{qn_0\mu} > t_{tr} = \frac{d}{\mu E}$.

In cases where the measurement is done at low enough electric field such that the free charge density, or doping level, is significant a TOF measurement would over estimate the mobility.

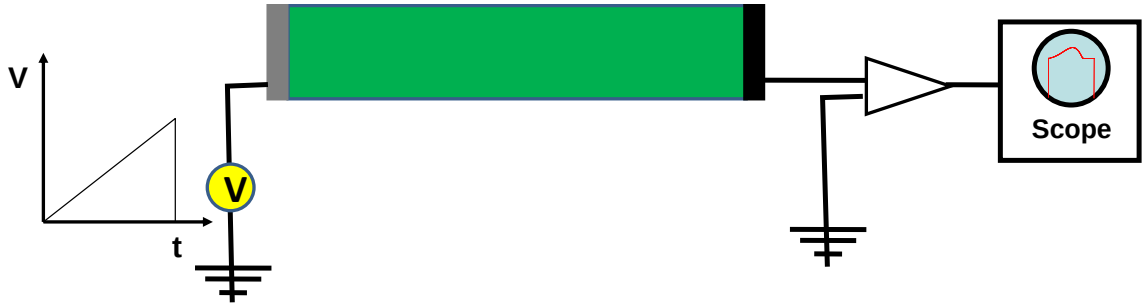

Figure 7. Schematic of the CELIV set-up

As is discussed above, the presence of free carriers (n_0) makes the TOF method not so reliable and hence a method that relies on the presence of these carriers could be a nice substitute. Such a substitute is the carrier extraction by a linearly increasing voltage (CELIV) method. [7-9] To create some basic intuition for the CELIV method we present in Figure 8 and Figure 9 results of a numerical simulation of a 1μm long device subject to a voltage sweep (V=A*t). In the simulations we test 3 cases of 3 different doping (n_0) levels. Figure 8 shows the current response to the applied voltage. We note that the response is composed of two parts superimposed on each other: a) a step function b) a single peak response. The first part (step function) is independent of the doping level

while the second feature is strongly dependent on the doping (free charge) density. As we will se below, the step function is associated with the geometrical capacitance (c) of the device (I=c*dV/dt=c*A) and the second feature is associated with the free charges being swept out of the device.

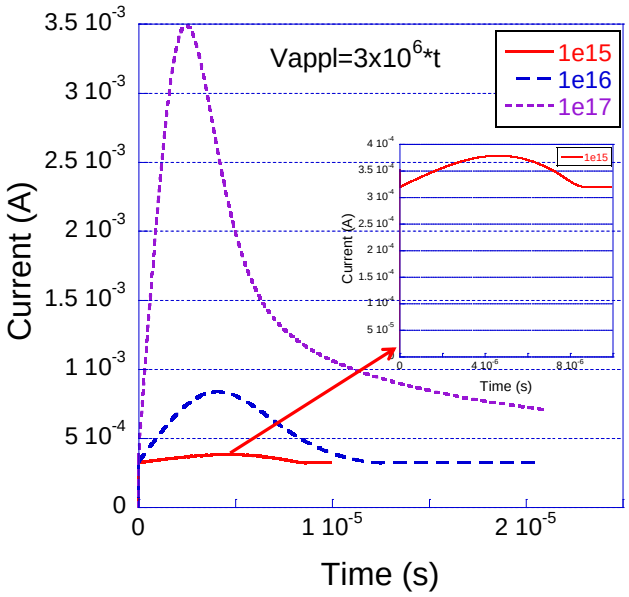

Figure 8. Simulated current response in a CELIV measurements for 3 different doping (n_0) levels.

The parameter set used in the simulation is:

Parameter	**Value**	
Length	d=1000nm	
Bias	A*t	
Cathode	$n_e(0,t)=10^{10}cm^{-3}$ $n_h(0,t)=10^{10}cm^{-3}$	
Anode	$n_e(d,t)=10^{10}cm^{-3}$ $n_h(d,t)=10^{10}cm^{-3}$	
Electron mobility	$\mu_e=10^{-4}cm^2/Vs$	
Hole mobility	$\mu_h=10^{-4}cm^2/Vs$	
Total density of states	$10^{21}cm^{-3}$	
Doping density	$10^{15},10^{16},10^{17}$ cm^{-3}	

Figure 9 shows the electric field and charge density distribution sampled at the time where the response is at its peak ($t=t_{max}$). Above each graph we show schematically the immobile dopant (+) and the remaining free charge (-). In this figure the applied electric field sweep the electrons from left to right leaving a depletion zone starting at x=0.
The shape of the current induced by the moving charges can be rationalized as follows. At first, as the voltage increases the carriers experience a higher electric field and hence move faster (higher current). As depletion zone starts to build up two effects take place: a) the total number of charges drifting in the device gets smaller b) if the doping is not

very small (above ~10^{16}cm^{-3}) , the electric field affecting the charges gets screened. Indeed, in Figure 9, for $n_{e0}=10^{17}$cm^{-3} $l(t_{max})$ is significantly shorter and as Figure 8 shows it results in t_{max} being smaller for this doping density.

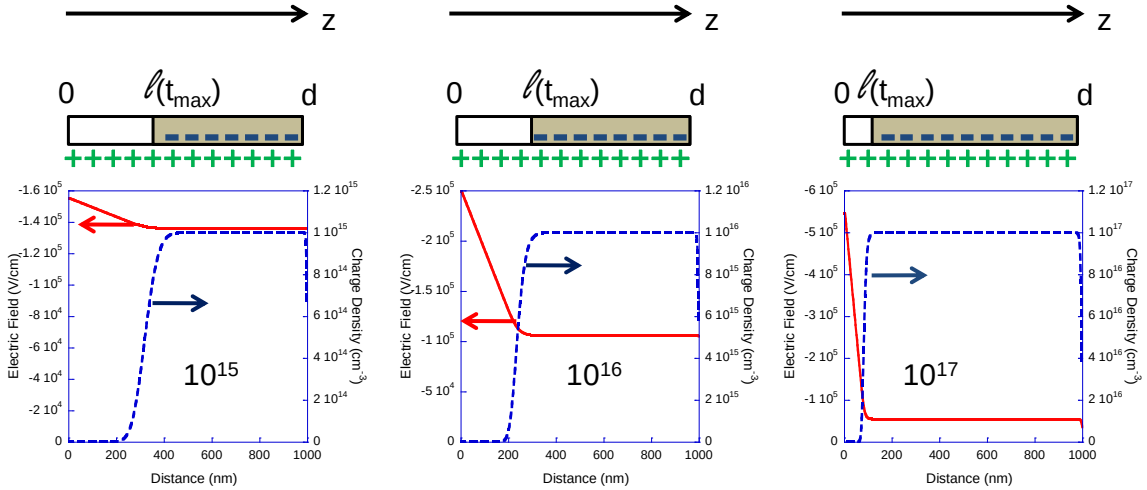

Figure 9. The electric field (full line) and charge density (dashed line) distribution for the three doping concentrations and sampled at t_{max}.

The above results, that were produced numerically, can be analyzed analytically [7]. We first write the applied potential that linearly ramps up the electric field as:

$$V(t) = -\int_0^d E(z,t)dz = At$$

As Figure 9 suggests the application of external field causes the charge density to shift away from the blocking contact and exit at the opposite contact. For the following derivation we'll assume n type doping at a level n_{e0}. The overall charge (i.e. exposed dopants) in the device as a function of time can be written as:

(19) $$Q(t) = qn_{e0}l(t) = \varepsilon\varepsilon_0\Delta E = \varepsilon\varepsilon_0\left[E(l,t) - E(0,t)\right] = \varepsilon\varepsilon_0\left[E(d,t) - E(0,t)\right]$$

Using the convention of Figure 1 and equation (7), the current due to the carriers drifting out through the contact at x=d is:

(20) $$j_{drift} = -q\mu_e n_{e0}E(d,t)$$

And it is also equal to the rate at which the charge is accumulated in the device:

(21) $$j_{drift} = -q\mu_e n_{e0}E(d,t) = \frac{dQ(t)}{dt} = qn_{e0}\frac{dl(t)}{dt}$$

Due to the electric field distribution in the CELIV scenario (see Figure 9) the voltage across the device can be written as:

$$
\begin{aligned}
V(t) = At &= -\int_0^d E(z,t)dz = -\int_0^l E(z,t)dz - \int_l^d E(z,t)dz = \\
&= -\int_0^l \left(E(0,t) + \frac{E(l,t)-E(0,t)}{l} z \right) dz - \int_l^d E(d,t)dz = \\
&= -\left(E(0,t)l(t) + \frac{E(d,t)-E(0,t)}{2} l(t) + \left(d - l(t)\right) E(d,t) \right) = \\
&= -\left(d \cdot E(d,t) - \frac{E(d,t)-E(0,t)}{2} l(t) \right)
\end{aligned}
\tag{22}
$$

Combining (19) to (22):

$$
\begin{cases}
qn_{e0} l(t) = \varepsilon\varepsilon_0 \left[E(d,t) - E(0,t) \right] \\
\dfrac{dl(t)}{dt} = -\mu_e E(d,t) \\
At = -\left[E(d,t) \cdot d - \dfrac{E(d,t)-E(0,t)}{2} \cdot l(t) \right]
\end{cases}
\tag{23}
$$

From these one arrives at the differential equation for l(t):

$$At = -\left[-\frac{1}{\mu_e} \frac{dl(t)}{dt} \cdot d - \frac{qn_{e0}}{2\varepsilon\varepsilon_0} \cdot l^2(t) \right]$$

Or:

$$\frac{dl(t)}{dt} = \frac{\mu_e A t}{d} - \frac{q\mu_e n_{e0}}{2\varepsilon\varepsilon_0 d} l^2(t) \tag{24}$$

The current through the device is composed of a displacement (capacitance) current and a drift current:

$$-j(t) = \varepsilon\varepsilon_0 \frac{d}{dt} E(z,t) + q\mu_e n_e(z,t) E(z,t) \tag{25}$$

Integrating over d:

$$j(t) = +\frac{\varepsilon\varepsilon_0 A}{d} - \frac{q\mu_e n_{e0}}{d} \int_{l(t)}^d E(z,t)dz = +\frac{\varepsilon\varepsilon_0 A}{d} - \frac{q\mu_e n_{e0}}{d} E(d,t)\left[d - l(t) \right] \tag{26}$$

Replacing E(d,t) according to $E(d,t) \cdot d = -At + \dfrac{E(d,t)-E(0,t)}{2} \cdot l(t) = -At + \dfrac{qn_{e0} l(t)}{2\varepsilon\varepsilon_0} l(t)$

the equation for the current is:

$$\boxed{j(t) = \frac{\varepsilon\varepsilon_0 A}{d} + q\mu_e n_{e0} \left(1 - \frac{l(t)}{d} \right) \left(\frac{At}{d} - \frac{qn_{e0}}{2\varepsilon\varepsilon_0 d} l^2(t) \right)} \tag{27}$$

From the above one can derive:

$$q\mu n_0 = \varepsilon\varepsilon_0 \left. \frac{d\left[j(t) / j(0) \right]}{dt} \right|_{t=0}$$

$$\varepsilon\varepsilon_0 = j(0)\frac{d}{A}$$

$$(28)\ t_{\max} = \sqrt[3]{\frac{\varepsilon\varepsilon_0 d^2}{qn_{e0}A\mu_e^2}}$$

Namely, using this simple method one can extract ε, μ, and the residual doping level n.

If the measurement is done fast enough, such that the drift current is significantly smaller compared to the displacement current than:

$$\frac{q\mu_e n_{e0}}{2d}l^2(t) \ll \frac{\mu_e t\varepsilon\varepsilon_0 A}{d}$$

Which leads to:

$$\frac{dl(t)}{dt} = \frac{\mu_e A}{d}t$$

$$dl(t) = \frac{\mu_e A}{d}tdt$$

$$l = \frac{\mu_e A}{2d}t^2$$

And the simplified expression reads:

$$(29)\ \begin{cases} j(t) = \dfrac{A}{d}\left[\varepsilon\varepsilon_0 + \sigma t\left(1 - \dfrac{\mu_e A t^2}{2d^2}\right)\right] & t < d\sqrt{\dfrac{2}{\mu_e A}} = t_{tr} \\ j(t) = \dfrac{A}{d}\varepsilon\varepsilon_0 & t > t_{tr} \end{cases}$$

$$(30)\ t_{\max} = d\sqrt{\frac{2}{3\mu_e A}}$$

And

$$\Delta J = J_{\max} - J(0) = J(0)\frac{dq}{\varepsilon\varepsilon_0}\sqrt{\frac{8\mu_e}{27A}}\cdot n_{e0}$$

IV.A. Field dependent mobility

As the above was developed for field independent mobility we will test numerically if the method can also be safely applied in cases where a field dependence exists. In Figure 10 we show simulation results of a device characterized by a field independent mobility of 10^{-4}cm^2/Vs (dashed line) and of one characterized by $\mu_e = 10^{-4}\exp\left(\gamma\sqrt{E}\right)cm^2V^{-1}s^{-1}$ with γ= 4.4e-3 (full line). In both cases the voltage sweep is and the doping level is 10^{15}cm^{-3}. Note the change in the curvature of the rising and falling edges which is a signature of field dependent mobility.

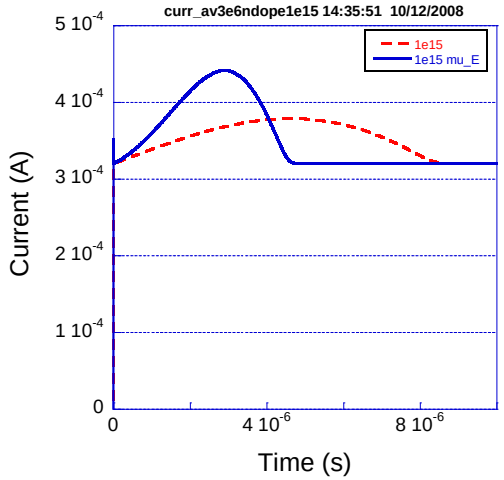

Figure 10. Simulated current response in a CELIV measurement. Dashed line is for a fixed mobility and the full line is for a field dependent mobility.

Next, we ran the simulation for several sweep rates (see Figure 11) and used the field at t_{max} as the relevant one to relate the mobility to (equation (30)).

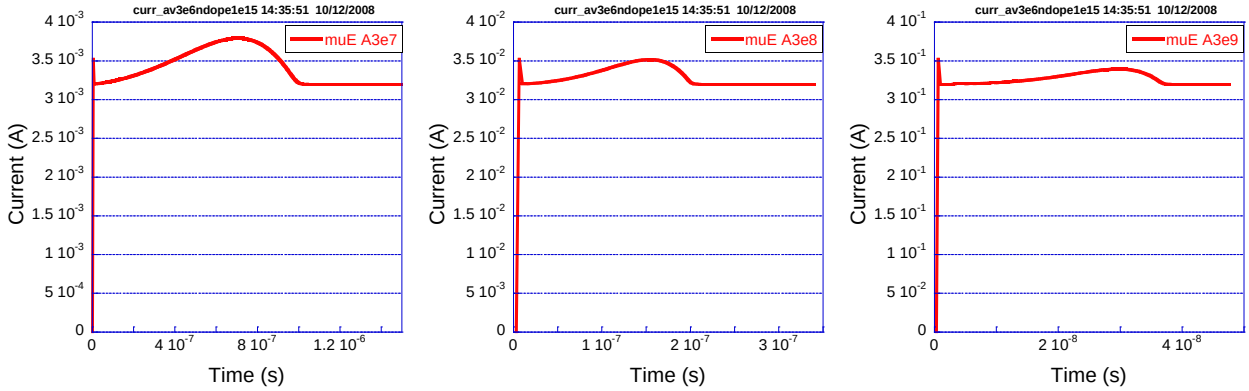

Figure 11. Simulated current response in a CELIV measurement for 3 sweep rates (3e7, 3e8, 3e9 V/s).

The results of the analysis is shown in Table I and we note the method underestimates the mobility and that the deviation increases as the field at which the mobility is deduced increases. As one would expect, the position of the maximum is dependent on the earlier part of the sweep where the mobility is lower and hence the increasing deviation. By fitting the extracted mobility we found γ to be 3.6e-3 instead of 4.4e-3. For such a simple method the accuracy of the method is not bad at all!!

Table I.

Applied Voltage at t_{max}	Applied field at t_{max}	Actual mobility at t_{max}	Extracted mobility	ratio
1V	1e4	1e-4	1e-4	1

8.7V	8.70E+04	3.66e-4	2.64e-4	0.72
21.3 V	2.10E+05	7.6e-4	4.4e-4	0.58
46.5V	4.65E+05	2e-3	9.25e-4	0.46
90V	9.00E+05	6.5e-3	2.5e-3	0.38

V. Step function excitation

In the following we make extensive use of the ideas and formulations presented in the book by Kao and Hwang [2] which is unfortunately long out of print. Let's assume the voltage to be a step function of the form:

$$(31)\quad V(t)=\begin{cases}0 & t<0\\ V & t\geq 0\end{cases}$$

Let's assume the charge carriers are electrons (n_e) such that equation (7) can be written as:

$$(32)\quad -j(z,t)=\varepsilon\varepsilon_0\frac{d}{dt}E(z,t)+q\mu_e n_e(z,t)E(z,t)+qD_e\frac{d}{dx}n_e(z,t)$$

And Poisson equation (3) takes the form:

$$(33)\quad \frac{dE}{dz}=-\frac{q}{\varepsilon\varepsilon_0}\left[n(z,t)-n_{e0}\right]$$

Integrating (32) while remembering equation (8):

$$\begin{aligned}-j(t)&=-\frac{1}{d}\int_0^d j(z,t)dz=\frac{1}{d}\int_0^d\left\{\varepsilon\varepsilon_0\frac{d}{dt}E(z,t)+q\mu_e n_e(z,t)E(z,t)+qD_e\frac{d}{dz}n_e(z,t)\right\}dz\\ &=-\frac{\varepsilon\varepsilon_0}{d}\frac{d}{dt}V+\frac{1}{d}\int_0^d\left\{-\mu_e\varepsilon\varepsilon_0\frac{dE(z,t)}{dz}E(z,t)+qD_e\frac{d}{dz}n_e(z,t)\right\}dz=\\ &=-\frac{\varepsilon\varepsilon_0}{d}\frac{d}{dt}V-\frac{\mu_e\varepsilon\varepsilon_0}{2d}\left[E^2(d,t)-E^2(0,t)\right]+\frac{qD_e}{d}\left[n_e(d,t)-n_e(0,t)\right]=\\ &=-\frac{\varepsilon\varepsilon_0}{d}\frac{d}{dt}V-\frac{\mu_e\varepsilon\varepsilon_0}{2d}\left[E^2(d,t)-E^2(0,t)\right]-\frac{\varepsilon\varepsilon_0 D_e}{d}\left[\left.\frac{dE(z,t)}{dz}\right|_{z=d}-\left.\frac{dE(z,t)}{dz}\right|_{z=0}\right]\end{aligned}\quad (34)$$

And finally:

$$(35)\quad j(t)=\frac{\varepsilon\varepsilon_0}{d}\frac{d}{dt}V+\frac{\mu_e\varepsilon\varepsilon_0}{2d}\left[E^2(d,t)-E^2(0,t)\right]+\frac{\varepsilon\varepsilon_0 D_e}{d}\left[\left.\frac{dE(z,t)}{dz}\right|_{z=d}-\left.\frac{dE(z,t)}{dz}\right|_{z=0}\right]$$

We also note that:

$$(36)\quad E(d,t)=E(0,t)+\frac{Q(t)}{\varepsilon\varepsilon_0}$$

Where $Q(t)=-q\int_0^d n_e(z,t)dz$ is the total amount of charge stored in the device at time t.

V.A. Contact limited current transients

We assume that the contact limits the charge density at the contact interface to a level that is too low to affect the electric field:

(37) $|Q| = qn_e(0,t) * d < V\frac{\varepsilon\varepsilon_0}{d}$

To have a feeling for the dynamics behind the device response we present numerical simulation results of a response to a voltage step of 40V of a device being 1000nm long. The mobility is taken to be 10^{-6}cm^2/Vs and the density at the cathode interface is ~2x10^{14}cm^{-3} (see Figure 12). The main graph shows the current response and the surrounding ones show snap shots of the charge distribution at different points in time, as marked with arrows.

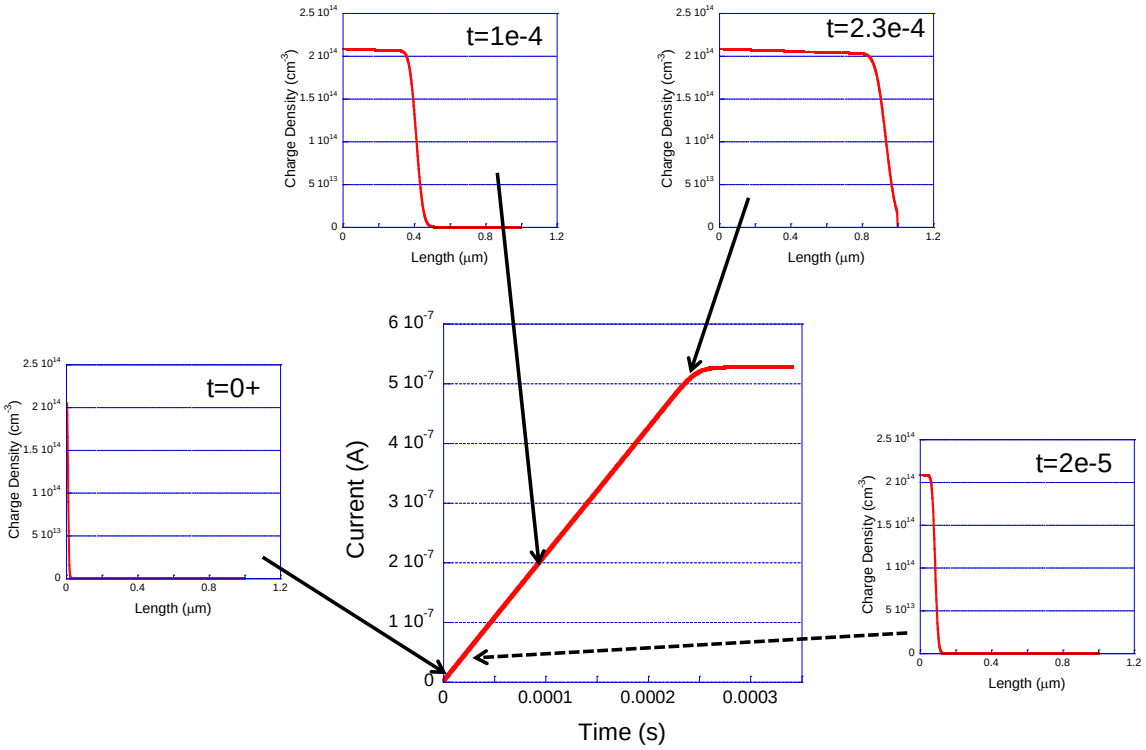

Figure 12. Simulated current response to a step function voltage excitation in device having high contact barrier. The surrounding figures show snap shots of the charge density distribution at the marked points in time.

The parameter set used in the simulation is:

Parameter	**Value**	
Length	d=1000nm	
Bias	V=40V	
Cathode	$n_e(0,t)=10^{14}$cm^{-3} $n_h(0,t)=10^{10}$cm^{-3}	
Anode	$n_e(d,t)=10^{10}$cm^{-3} $n_h(d,t)=10^{10}$cm^{-3}	
Electron mobility	$\mu_e=10^{-6}$cm^2/Vs	
Hole mobility	$\mu_h=10^{-6}$cm^2/Vs	
Total density of states	10^{21}cm^{-3}	
Doping density	none	

As Figure 12 shows, the current is rising linearly with time as the device is being filled with charges. Once the charges reach the anode, the device is full and the current response flattens.

To rigorously analyze the response we remember that under the physical conditions assumed here we can typically also neglect diffusion currents and hence equation (35) can be written as:

$$(38)\quad j(t)=\frac{\varepsilon\varepsilon_0}{d}\frac{d}{dt}V+\frac{\mu_e\varepsilon\varepsilon_0}{2d}\left[E^2(d,t)-E^2(0,t)\right]\overset{t>0}{=}\frac{\mu_e\varepsilon\varepsilon_0}{2d}\left[E^2(d,t)-E^2(0,t)\right]$$

And using (36):

$$(39)\quad j(t)\overset{t>0}{=}\frac{\mu_e Q(t)}{2d}\left[2E(d,t)-\frac{Q(t)}{\varepsilon\varepsilon_0}\right]=\frac{\mu_e Q(t)}{2d}\left[2E(0,t)+\frac{Q(t)}{\varepsilon\varepsilon_0}\right]$$

As we assumed the charge density to be low $\left(|Q|\ll V\frac{\varepsilon\varepsilon_0}{d}\right)$:

$$(40)\quad j(t)\overset{t>0}{=}\frac{\mu_e Q(t)}{2d}2E(0,t)=-\frac{\mu_e Q(t)}{d}\frac{V}{d}=-\frac{\mu_e Q(t)V}{d^2}=-\frac{Q(t)}{\tau_{tr}}=\frac{q\int_0^d n_e(z,t)dz}{\tau_{tr}}$$

To find *Q(t)* we rewrite equation (1) neglecting diffusion and generation/recombination:

$$(41)\quad \frac{\partial}{\partial t}n_e(z,t)=\frac{\partial}{\partial z}\left[\mu_e n_e(z,t)E(z,t)\right]$$

The assumption of the charge density being low $\left(|Q|\ll V\frac{\varepsilon\varepsilon_0}{d}\right)$ allows us to deduce that

$\frac{\partial}{\partial z}\left[\mu_e E(z,t)\right]=0$ and hence:

$$(42)\quad \frac{\partial}{\partial t}n_e(z,t)=\mu_e E\frac{\partial}{\partial z}n_e(z,t)$$

And finally the differential equation for the total charge density Q is:

$$(43)\quad \frac{\partial}{\partial t}Q(t)=-q\frac{\partial}{\partial t}\int_0^d n_e(z,t)dz=-q\mu_e E\int_0^d\frac{\partial}{\partial z}n_e(z,t)=-q\mu_e E\left[n_e(d,t)-n_e(0,t)\right]$$

The boundary conditions are $n_e(0,t)=n_e(0)$ and $Q(0)=0$.

From the above we deduce the charge density at the anode to be:

$$(44)\, n_e(d,t)=\begin{cases}0 & t<\tau_{tr}\\ n_e(0) & t\geq\tau_{tr}\end{cases}$$

And the total charge density can thus be written as:

$$Q(t)=\begin{cases}q\mu_e E n_e(0)t & t<\tau_{tr}\\ q\mu_e E n_e(0)\tau_{tr} & t\geq\tau_{tr}\end{cases}=\begin{cases}q\mu_e\frac{V}{d}n_e(0)t & t<\tau_{tr}\\ qdn_e(0) & t\geq\tau_{tr}\end{cases}$$

Inserting into equation (40) we arrive at the expression for the current:

$$(45)\quad j(t)=\begin{cases}\dfrac{q\mu_e V n_e(0)t}{\tau_{tr}d} & t<\tau_{tr}\\ \dfrac{q\mu_e V n_e(0)}{d} & t\geq\tau_{tr}\end{cases}$$

In this case finding the mobility can be done by locating the crossing between the slopes ($t=\tau_{tr}$) and applying

$$(46)\quad \mu_e=\frac{d^2}{\tau_{tr}V}$$

V.B. Space charge limited current transient

We assume here the charge density that can be supplied by the contacts is high

(47) $|Q| = qn_e(0,t) * d > V\frac{\varepsilon\varepsilon_0}{d}$.

To have a feeling for the carrier and field distribution dynamics we present numerical simulation results of a response to a voltage step of 40V of a device being 300nm long. The mobility is taken to be 10^{-6}cm^2/Vs and the density at the cathode interface is 10^{19}cm^{-3} (see Figure 13). The main graph shows the current response and the surrounding ones show snap shots of the charge distribution and electric field at different points in time, as marked with arrows (note the electric field axis is reversed).

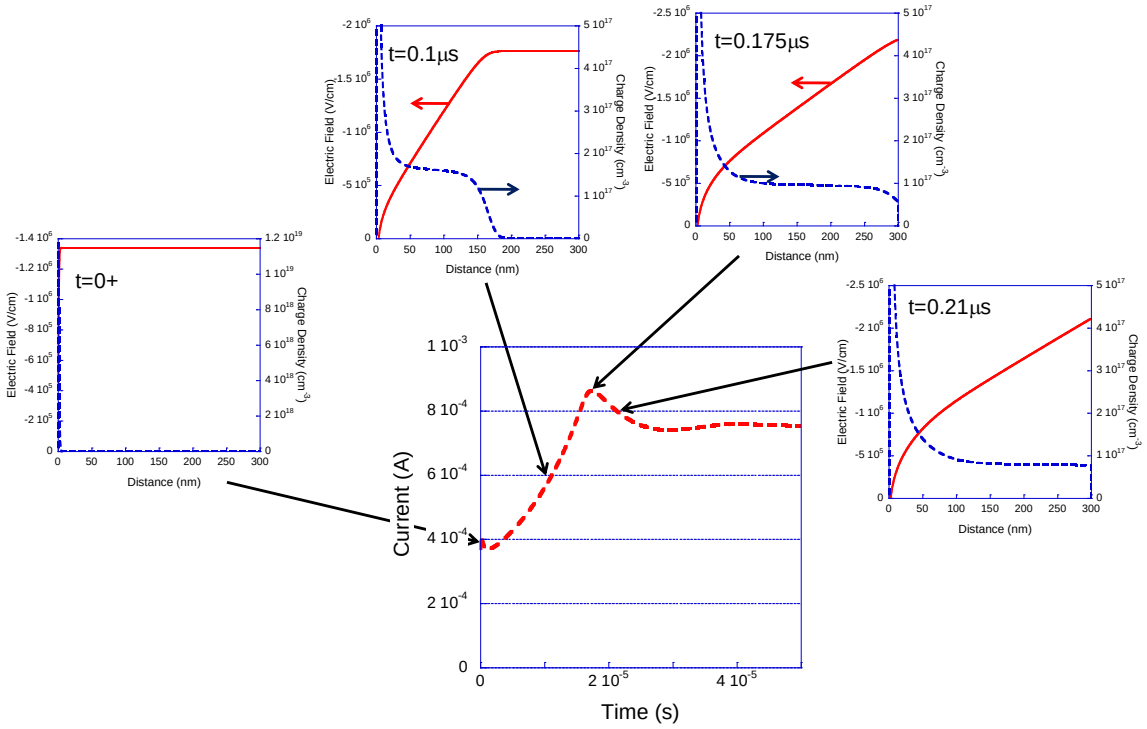

Figure 13. Current response to a voltage step of 40V of a device being 300nm long. The mobility is taken to be 10^{-6}cm^2/Vs and the density at the cathode interface is 10^{19}cm^{-3}. The main graph shows the current response and the surrounding ones show snap shots of the charge distribution and electric field at different points in time, as marked with arrows (note the electric field axis is reversed).

The parameter set used in the simulation is:

Parameter	**Value**	
Length	d=300nm	
Bias	V=40V	
Cathode	$n_e(0,t)=10^{19}$cm^{-3} $n_h(0,t)=10^{10}$cm^{-3}	
Anode	$n_e(d,t)=10^{10}$cm^{-3} $n_h(d,t)=10^{10}$cm^{-3}	

Electron mobility	$\mu_e=10^{-6}cm^2/Vs$	
Hole mobility	$\mu_h=10^{-6}cm^2/Vs$	
Total density of states	$10^{21}cm^{-3}$	
Doping density	none	

As the injection contact is the cathode, at z=0, it is common to assume:

(48) $E(0^+,t)\cong 0$

And we note that this is supported by the numerical results shown in Figure 13. Inserting (48) into (35) we get:

(49) $j(t)=\frac{\mu_e\varepsilon\varepsilon_0}{2d}E^2(d,t)-\frac{\varepsilon\varepsilon_0 D_e}{d}\left.\frac{dE(z,t)}{dz}\right|_{z=0}=\frac{\mu_e\varepsilon\varepsilon_0}{2d}E^2(d,t)+\frac{qD_e}{d}n_e(0,t)$

Assuming $\frac{\mu_e\varepsilon\varepsilon_0}{2d}E^2(d,t)\gg\frac{qD_e}{d}n_e(0,t)$:

(50) $j(t)=\frac{\mu_e\varepsilon\varepsilon_0}{2d}E^2(d,t)$

The above assumption can also be written as $\frac{V}{kT/q}\gg 2\left(qn_e(0,t)\cdot d\right)/\left(V\frac{\varepsilon\varepsilon_0}{d}\right)$ which together with equation (47) implies:

(51) $\frac{V}{kT/q}\gg 1$

This condition is usually replaced by saying that diffusion is being neglected.

Another expression for the current can be derived by considering that until the charge front reaches the anode ($t<\tau_{tr}$) the current at the anode interface is displacement current only:

(52) $j(t)=j(d,t)=-\varepsilon\varepsilon_0\frac{d}{dt}E(d,t)$

Combining (50) and (52) we get for $t<\tau_{tr}$:

(53) $\frac{d}{dt}E(d,t)=-\frac{\mu_e}{2d}E^2(d,t)$

To solve (53) we add the boundary condition at t=0 - $E(d,0)=-\frac{V}{d}$.

The solution takes the form: $E(d,t)=E(d,0)\left(1+\frac{t}{t_1}\right)^{-1};t_1=\left(E(d,0)\frac{\mu_e}{2d}\right)^{-1}$ which is equivalent to:

$$E(d,t)=E(d,0)\left(1-\frac{t}{2\tau_0}\right)^{-1};-2\tau_0=2\frac{d}{\mu_e E(d,0)}$$

$$(54)\quad E(d,t) = -\frac{V}{d}\left(1-\frac{t}{2\frac{d^2}{\mu_e V}}\right)^{-1} \quad ;2\tau_0 = 2\frac{d^2}{\mu_e V}$$

Inserting (54) into (52):

$$(55)\quad j(t) = j(d,t) = -\varepsilon\varepsilon_0 \frac{d}{dt}\left\{-\frac{V}{d}\left(1-\frac{t}{2\frac{d^2}{\mu_e V}}\right)^{-1}\right\}$$

And finally, for $t<\tau_{tr}$, we get:

$$(56)\quad j(t) = \varepsilon\varepsilon_0 \frac{\mu_e V^2}{2d^3}\left(1-\frac{t}{2\frac{d^2}{\mu_e V}}\right)^{-2} \quad ; \quad t < \tau_{tr}$$

To find τ_{tr} we use the fact that the carrier front is experiencing the same field as at the anode (see Figure 13):

$$d = \int_0^{\tau_{tr}} -\mu_e E(d,t)dt = \mu_e \frac{V}{d}\int_0^{\tau_{tr}}\left(1-\frac{t}{2\frac{d^2}{\mu_e V}}\right)^{-1} dt = \mu_e \frac{V}{d}\int_0^{\tau_{tr}}\left(\frac{2\frac{d^2}{\mu_e V}}{2\frac{d^2}{\mu_e V}-t}\right)dt$$

$$d = \mu_e \frac{V}{d} 2\frac{d^2}{\mu_e V}\int_0^{\tau_{tr}}\left(\frac{1}{2\frac{d^2}{\mu_e V}-t}\right)dt = 2d\cdot\left\{\ln\left(2\frac{d^2}{\mu_e V}\right)-\ln\left(2\frac{d^2}{\mu_e V}-\tau_{tr}\right)\right\} = -2d\ln\left(1-\tau_{tr}/\left(2\frac{d^2}{\mu_e V}\right)\right)$$

hence:

$$(57)\quad \tau_{tr} = 2\left(1-e^{-\frac{1}{2}}\right)\frac{d^2}{\mu_e V} = 2\left(1-e^{-\frac{1}{2}}\right)\tau_0 \simeq 0.786\tau_0$$

Namely, the peak of the current takes place at $t = \tau_{tr} = 0.786\frac{d^2}{\mu_e V}$ or the mobility can be found from:

$$(58)\quad \mu_e = 0.786\frac{d^2}{\tau_{tr} V}$$ where the electric field related to this mobility is in the range of [V/d, 1.5V/d].

One way to ensure that the device is operating within the physical picture used in this section is to verify that the shape of the current profile is similar to the one shown in Figure 13. To assist this we compute the following:

$$\frac{j(0)}{j(\infty)} = \frac{\varepsilon\varepsilon_0 \dfrac{\mu_e V^2}{2d^3}}{\dfrac{9}{8}\varepsilon\varepsilon_0\mu_e \dfrac{V^2}{d^3}} = \frac{4}{9} = 0.44$$

$$\frac{j(\tau_{tr})}{j(\infty)} = \frac{\varepsilon\varepsilon_0 \dfrac{\mu_e V^2}{2d^3}\left(1-\dfrac{0.786}{2}\right)^{-2}}{\dfrac{9}{8}\varepsilon\varepsilon_0\mu_e \dfrac{V^2}{d^3}} = \frac{4}{9}\left(1-\frac{0.786}{2}\right)^{-2} \simeq 1.2$$

To finalize this part we show in Figure 14 the current response for several types of contacts reflected by the boundary condition at the cathode, $n_e(0,t)$.

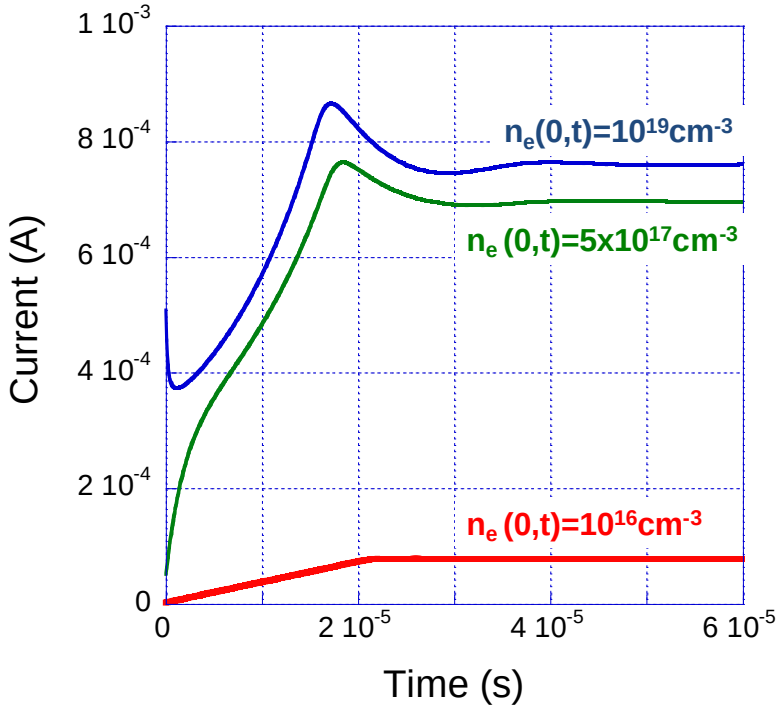

Figure 14. Current response as a function of the charge density supplied by the contact. Note that as the density is lowered from 10^{19}cm^{-3} to 10^{16}cm^{-3} the shape changes from SCLC type to contact limited type.

V.C. Optical step function excitation

The idea behind applying an optical step function excitation is to have a physical scenario similar to the one described in section V.A but with the boundary condition at the contact being a generation rate rather than a fixed charge density. By controlling the height of the step (i.e. the optical power) as well as by choosing different applied biases one can generate different steady state charge densities which would be equivalent to varying the barrier height in section V.A. Due to the relatively slow response time of organic LEDs one can use inorganic LEDs as the excitation source to produce ideal enough step function. Suitable experimental set-up is shown in Figure 15.

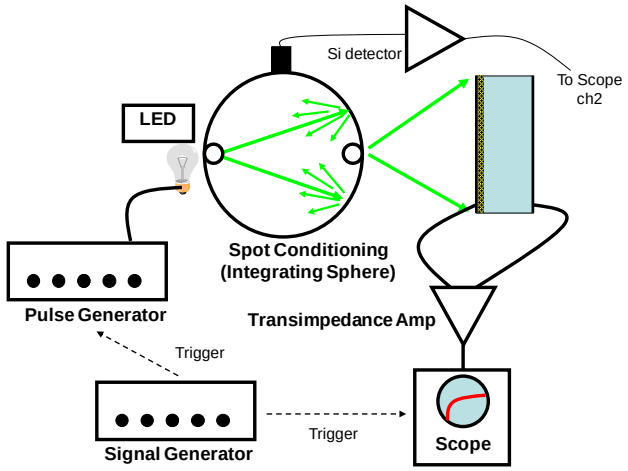

Figure 15. Schematic description of a suitable experimental set-up.

To have a feeling for the carrier distribution dynamics we present (Figure 16) numerical simulation results of a response to a step function optical excitation. The device was 1000nm long and biased at 40V. The mobility is taken to be 10^{-6}cm^2/Vs and the absorption depth is 100nm. The main graph shows the current response and the surrounding ones show snap shots of the electron distribution at different points in time, as marked with arrows. The first and last snap shots include also the hole's distribution in blue dashed line.

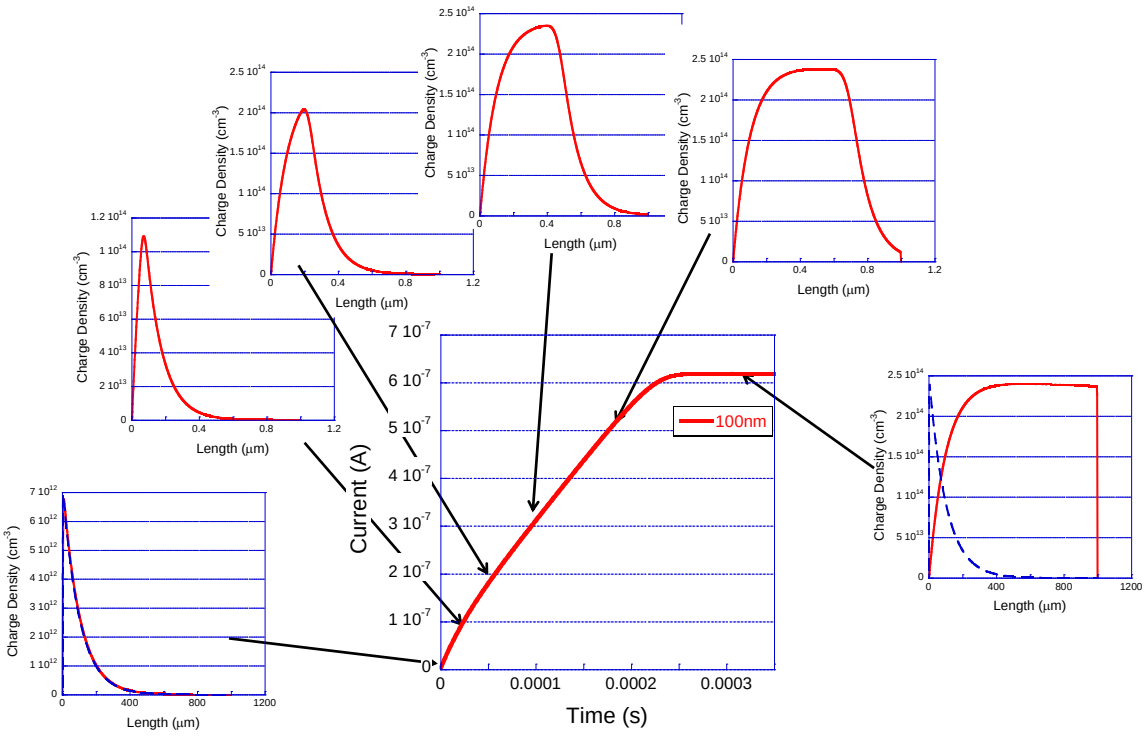

Figure 16. Current response to a light step of a device being 1000nm long and biased at 40V. The mobility is taken to be 10^{-6}cm^2/Vs and the absorption depth is 100nm. The main graph shows the current response and the surrounding ones show snap shots of the electron distribution at different points in time, as marked with arrows. The first and last snap shots include also the hole distribution in blue dashed line.

The parameter set used in the simulation is:

Parameter	**Value**	
Length	d=1000nm	
Absorption length	L_{abs}=100nm	
Bias	V=40V	
Cathode	$n_e(0,t)=10^{10}$cm^{-3} $n_h(0,t)=10^{10}$cm^{-3}	
Anode	$n_e(d,t)=10^{10}$cm^{-3} $n_h(d,t)=10^{10}$cm^{-3}	
Electron mobility	$\mu_e=10^{-6}$cm^2/Vs	
Hole mobility	$\mu_h=10^{-6}$cm^2/Vs	
Total density of states	10^{21}cm^{-3}	
Doping density	none	

V.C.1. Simple mathematical analysis

To simplify the analysis we assume that the absorption length is negligibly small. Under this assumption we can neglect the contribution of holes to the current and, in analogy to section V.A, we can rewrite equation (40):

$$(59)\quad j(t) \overset{t>0}{=} -\frac{\mu_e Q(t) V}{d^2} = -\frac{Q(t)}{\tau_{tr}} = \frac{q\int_0^d n_e(z,t)dz}{\tau_{tr}}$$

On the other hand, equation (42) must be rewritten to include a generation term

$$(60)\ \frac{\partial}{\partial t} n_e(z,t) = \mu_e E(z,t) \frac{\partial}{\partial z} n_e(z,t) + G(z,t)$$

Where our assumption of negligibly small absorption length leads to:

$$(61)\ G(z,t) = \begin{cases} G_0 & z = 0 \\ 0 & z > 0 \end{cases}$$

Under the assumption that diffusion currents are not important we can replace the boundary condition (61) with:

$$\frac{\partial}{\partial t} n_e(0,t) = -\mu_e \frac{V}{d} n_e(0,t) + G(0,t) = 0$$

Or:

$$(62)\quad n_e(0,t) = \frac{d \cdot G_0}{\mu_e V}$$

This brings us to the point where we can now use the results of section V.A using (62) as the boundary condition:

$$(63)\quad j(t) = \begin{cases} q\frac{t}{\tau_{tr}} G_0 & t < \tau_{tr} \\ qG_0 & t \geq \tau_{tr} \end{cases}$$

As before, finding the mobility can be done by locating the crossing between the slopes ($t=\tau_{tr}$) and applying

$$(64)\quad \mu_e = \frac{d^2}{\tau_{tr} V}$$

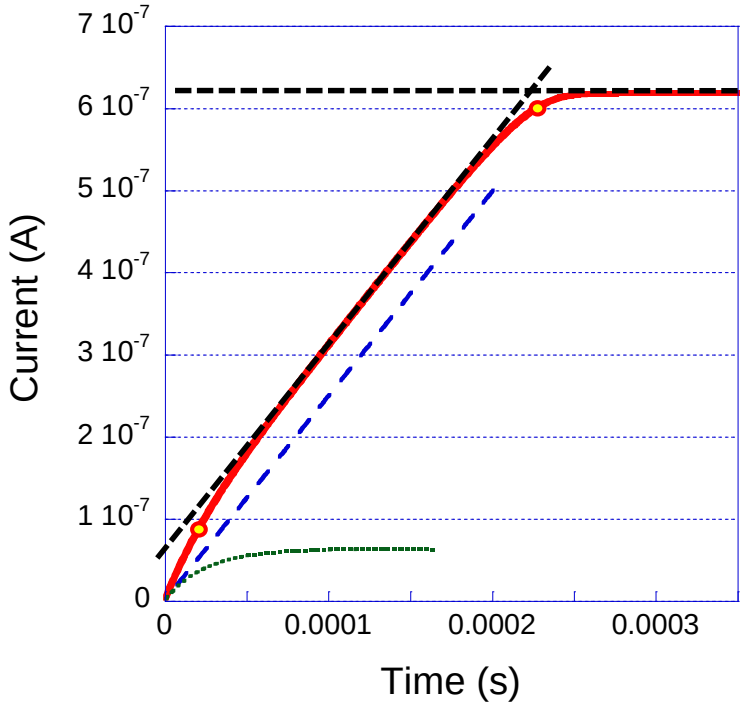

Figure 17. The response shown in Figure 16 (solid line), the slope of the long time response (dashed line), the short time response (dotted line). The yellow circles denote the points where the slope seems changes.

As Figure 17 shows, the response is almost identical in shape to the one shown in Figure 12 for a single carrier injection from a limiting contact. This similarity motivated us to simplify the analysis above by assuming very short absorption length and negligible contribution of holes to the current. We return now to these assumptions and we note the apparent difference in the existence of a faster slope at the very beginning. To isolate this additional feature we first fitted the slope of the long time linear rise (dashed line) and subtracted it from the full response to arrive at the response shown in dotted line.

To understand the origin of this additional feature we remember that the optical excitation is generating both electrons and holes and that for low enough excitation the two responses are almost independent.

Lifting the assumption of negligible contribution of holes to the current we rewrite (59):

$$(65)\quad j(t) \overset{t>0}{=} j_h(t) + j_e(t) = \frac{q\mu_h \int_0^d n_h(z,t)dz}{d^2} + \frac{q\mu_e \int_0^d n_e(z,t)dz}{d^2}$$

And if we recall that holes are extracted by the contact through which the light is shining we can assume that holes distribution would resemble the absorption profile (see also Figure 16):

$$n_h(z,t) = n_h(0,t)\exp\left(-\frac{z}{L_{abs}}\right)$$

and for $L_{abs} \ll d$

(66) $\int_0^d n_h(z,t)dz \cong L_{abs} n_h(0,t)$

Examining Figure 16 we can also write for the steady state:

(67) $\int_0^d n_e(z,t)dz \overset{t\gg}{\cong} d \cdot n_e(d,t)$

To supplement the above we note that at steady state there is no charging of the device. Namely, the rate at which holes exit the device at z=0 is equal to rate at which electrons exit at z=d:

(68) $\mu_h E n_h(0,t) = \mu_e E n_e(d,t)$

Combining (65) to (68) we find that for the steady state

$$\left.\frac{j_e(t)}{j_h(t)}\right|_{t\gg} \cong \frac{L_{abs}}{d}$$

We recall that the simulations were carried out for d=1μm and L_{abs}=100nm and indeed the response shown in Figure 17 with dotted line is about 10^{th} of the total response (i.e. it represents the contribution of holes to the current).

VI. Excitation of LEDs

VI.A. Time Domain.

The physical picture we will be concerned here is similar to the one described in ref [10]. We assume a step function voltage excitation resulting in double injection of electrons and holes from their respective contacts. We also assume that the one of the charge carriers is much faster than the other so that in the output EL we could expect to be able to differentiate between the contributions made by the transport of each type of carriers. Figure 18 shows results of numerical simulations of such scenario. In this simulation the electrons are 20 times faster than the holes (μ_h=0.05μ_e; μ_e =10^{-6}cm^2/Vs) and we would expect to start seeing light output once electrons reach the opposite contact and meet the holes that have hardly moved. The device length is d=100nm and the applied voltage is (V-Vbi)=5V. The contact barriers are set at 0.2eV making the injection not limited by the contact. Figure 18a shows the first 30μs and Figure 18b shows the long time response. The top curve (marked Rec) denotes the overall recombination (exciton generation) in the device which in the absence of any quenching effects would represent the light output. The curves marked Rec (5nm) and Rec (10nm) were calculated excluding the 5nm and 10nm close to the contacts, respectively. The curves surrounding the temporal response depict the charge distribution at the point in times marked with the arrows.

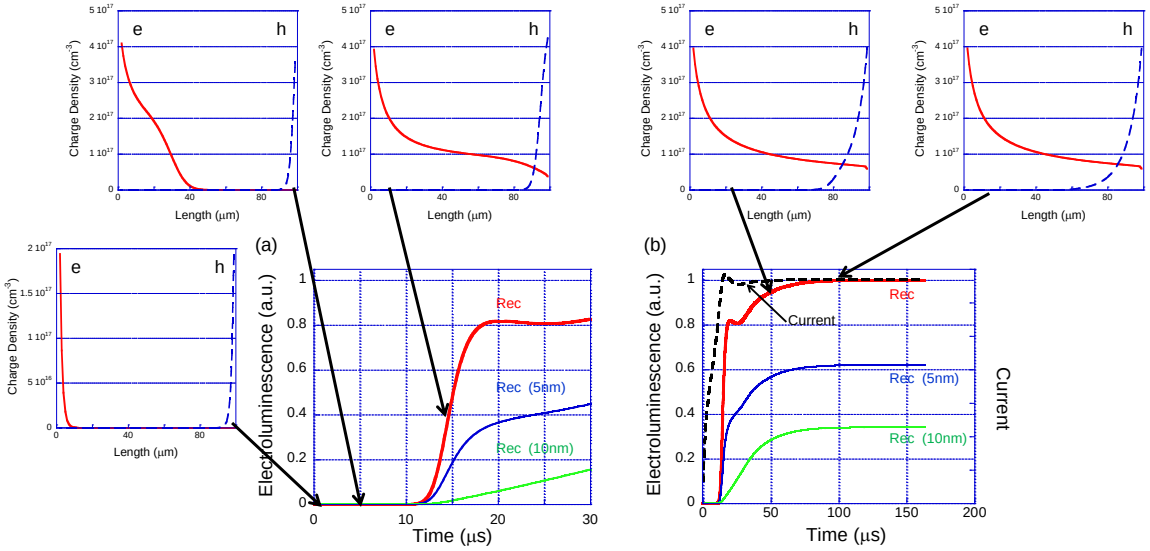

Figure 18.

VI.A.1. Simple mathematical analysis

For simplicity we will assume that one of the charge carriers is much faster than the other (as in Figure 18) and that the injection of these carriers is contact limited.

a) Analysis of the fast carriers

We attempt here to derive an expression describing the fast turn on of the electroluminescence that is associated with the fast carriers transport. Namely, the physical scenario is almost identical to the one described in section V.A. The only difference now is that we are interested in the light output which under the present assumptions corresponds to the charge density (of the fast carriers) at their exit contact. We recall equation (44)

$$(69)\ n_e(d,t) = \begin{cases} 0 & t < \tau_{tr} \\ n_e(0) & t \geq \tau_{tr} \end{cases}$$

And if we assume that the light emission is proportional to the charge recombination than:

$$(70)\ EL = B \cdot n_h(d,t) \cdot n_e(d,t)$$

Which for t not much lathe than the transit time of the fast carriers (electrons in the above equations):

$$(71)\ EL = B \cdot n_h(d) \cdot n_e(d,t) = \begin{cases} 0 & t < \tau_{tr} \\ B \cdot n_h(d) \cdot n_e(0) & t \geq \tau_{tr} \end{cases}$$

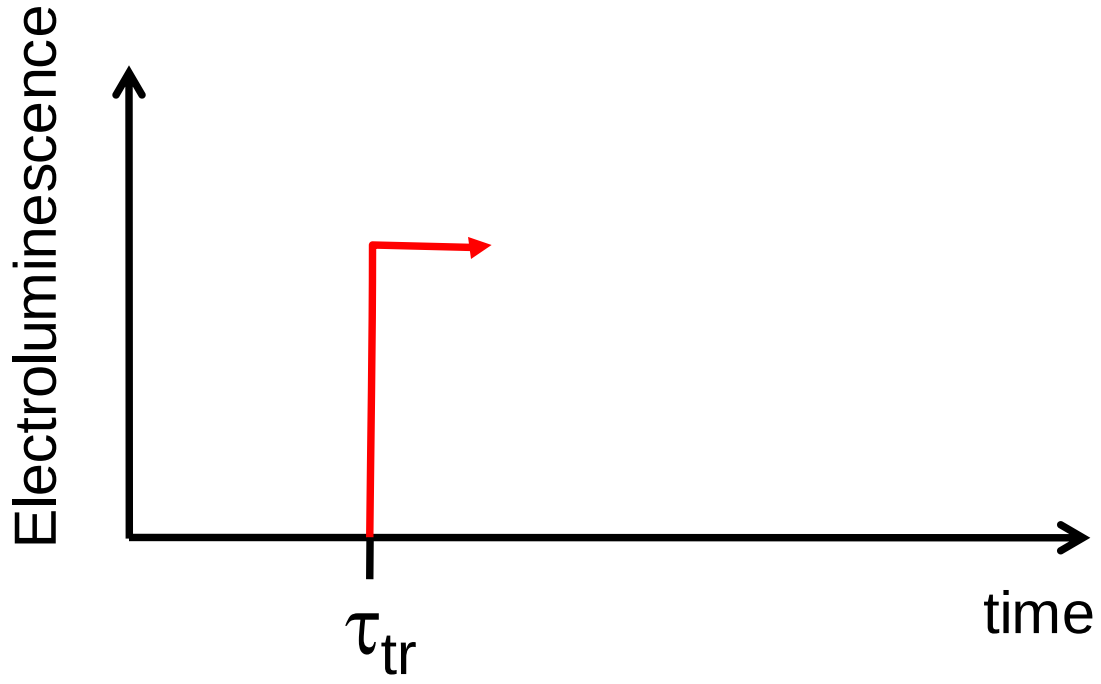

Figure 19. Schematic description of the EL as a function of time according to equation (71).

In real experiments the EL rise is not so sharp and can span time period that is of the order of τ_{tr} (see Figure 22). In such a case it becomes non trivial to define the transit time.

Do we choose the onset or the top of the step? In ref [10] this was answered with the aid of numerical simulation and we will try to approach it here in a somewhat more analytic manner.

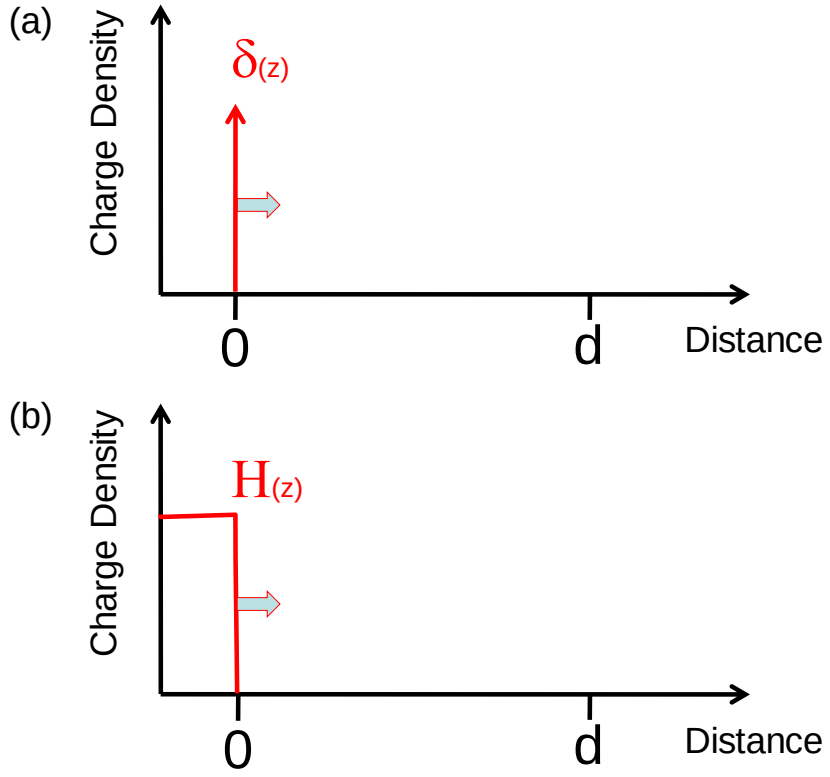

Figure 20. (a) Illustration of a delta function charge excitation which was studies in section III. (b) Illustration of a step function charge excitation which is studied in this section.

We first ignore the drift motion of the charges and deal only with diffusion. For the delta function excitation ($\delta_{(z)}$) we know the solution to be (see also equation (15)):

$$(72)\quad n_e(z,t) = \frac{n_{e0}}{2\sqrt{\pi D_e t}} e^{-\frac{z^2}{4D_e t}}$$

For the step function excitation ($H_{(z)}$) we can write the solution as a convolution with the response to a delta function:

$$(73)\quad n_e(z,t) = \int_{-\infty}^{\infty} \frac{n_{e0}}{2\sqrt{\pi D_e t}} e^{-\frac{s^2}{4D_e t}} H(z-s)ds = \frac{n_{e0}}{2\sqrt{\pi D_e t}} \int_{z}^{\infty} e^{-\frac{s^2}{4D_e t}} ds$$

Changing variables: $\frac{s}{2\sqrt{D_e t}} = k$

$$(74)\quad n_e(z,t)=\frac{n_{e0}}{\sqrt{\pi}}\int_{\frac{z}{2\sqrt{D_e t}}}^{\infty} e^{-k^2}dk = n_{e0}\left[\frac{1}{2}-\frac{1}{2}erf\left(\frac{z}{2\sqrt{D_e t}}\right)\right]$$

In analogy to equation (15) we add the drift velocity:

$$(75)\quad n_e(z,t)=n_{e0}\left[\frac{1}{2}-\frac{1}{2}erf\left(\frac{z-\mu_e\frac{V}{d}t}{2\sqrt{D_e t}}\right)\right]$$

And finally

$$(76)\quad EL=B\cdot n_h(d)\cdot n_e(d,t)=B\cdot n_h(d)\cdot n_{e0}\left[\frac{1}{2}-\frac{1}{2}erf\left(\frac{d-\mu_e\frac{V}{d}t}{2\sqrt{D_e t}}\right)\right]$$

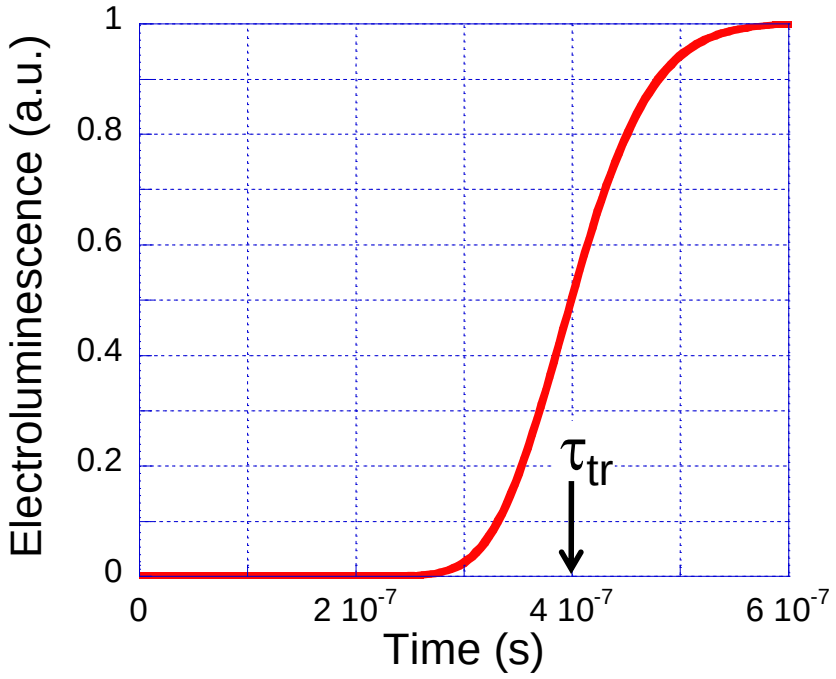

Figure 21. Calculation of equation (76) using μ=10^{-5}cm^2/Vs, d=100nm, V=2.5V, D=(kT/q)μ

As equation (76) and Figure 21 show, the transit time is to be measured at the point where the intensity reached half of its final value. Note that if one uses the onset time (~3x10^{-7}) the mobility would be overestimated and the effect would be more pronounced for short devices and low applied voltages.

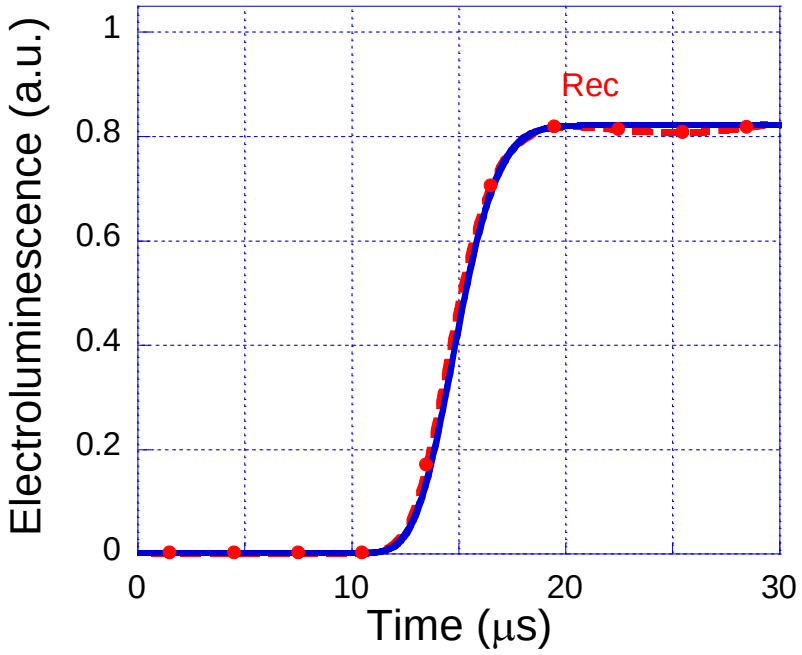

Figure 22. The short time EL response for a step function excitation of (V-Vbi)=5V shown in Figure 18 (dashed line, round symbols) and a fit using equation (76) (full line).

Figure 22 shows the simulated response presented in Figure 18 (dashed line, round symbols) and a fit using equation (76) (full line). The fit of equation (76) to the experimental curve results in $\mu_{fast} = 1.33 \cdot 10^{-6} cm^2 / Vs$, $D_{fast} = 1 \cdot \frac{kT}{q} \mu_{fast}$.

To show the application to experimental data we show in Figure 22 a fit to data similar to the one reported in ref. [10].

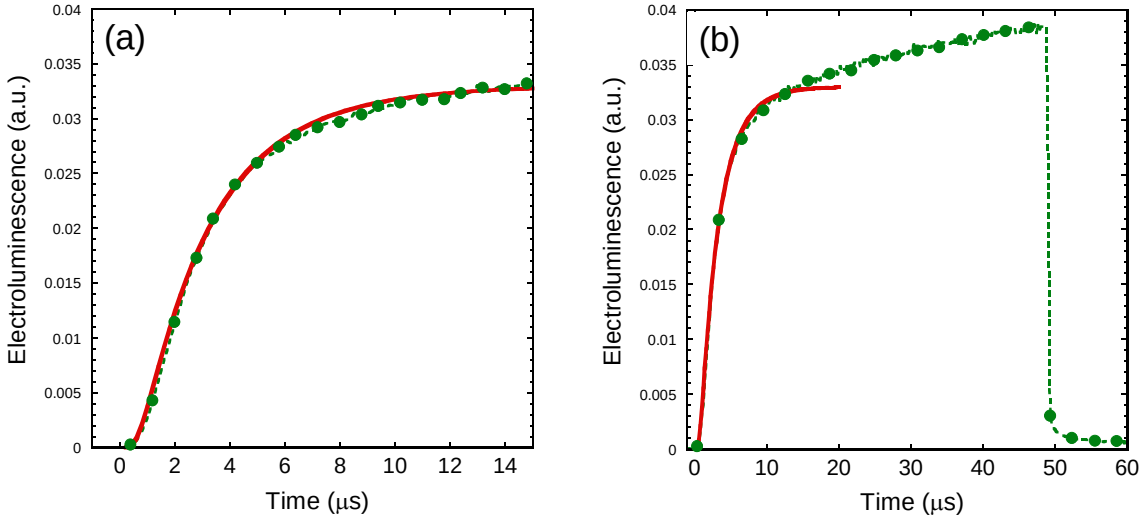

Figure 23. Measured EL response for a step function excitation of (V-Vbi)=3.1V applied to a LED having a thickness of d=75nm (round symbols). (a) The first 15μs (b) Longer time scale showing also the contribution of the slow carriers. The full line is a fit using equation (76). Device structure = (ITO/ PEDOT:PSS [50nm]/PPVcp[75nm]/Ca).

Figure 22 shows the response of a PPV co-polymer to a voltage step function excitation and the device structure was (ITO/ PEDOT:PSS [50nm]/PPVcp[75nm]/Ca). While we know that in this device the fast carriers are holes we will perform the analysis using the equations developed as if the electrons are the fast carriers. The fit of equation (76) to the experimental curve results in $\mu_{fast} = 7 \cdot 10^{-6} cm^2 / Vs$, $D_{fast} = 40 \cdot \frac{kT}{q} \mu_{fast}$. This anomalous enhancement of the diffusion constant (Einstein relation) seems too high to be due to the semiconductor being degenerate and is most likely due to spatial dispersion of the transport properties.[11-13]

b) Analysis of the slow carriers

In the previous section we defined the electrons as being the fast carriers hence we are now interested in the effect of the holes penetrating the device. The final density of the holes in the device can be limited by either of the following two:

1. Recombination with the electrons (i.e. zero hole leakage current)
2. Their front reaching the cathode and filling the entire device (i.e. high hole leakage current).

(1) High efficiency case

Starting with the high efficiency case, as is the simulated case presented in Figure 18, we rewrite equation (2) neglecting diffusion and generation:

(77) $$\frac{\partial}{\partial t} n_h(z,t) = -\mu_h(E) E(z,t) \frac{\partial}{\partial z} n_h(z,t) - R(z,t)$$

(78) $$\frac{\partial}{\partial t} \int_0^d n_h(z,t) dz = -\mu_h E \int_0^d \frac{\partial}{\partial z} n_h(z,t) dz - \int_0^d R(z,t) dz$$

Writing the recombination as a bi-molecular rate:

(79) $$\frac{1}{q} \frac{\partial}{\partial t} Q_h(t) = \mu_h \frac{V}{d} n_h(d,t) - \int_0^d B n_h(z,t) n_e(z,t) dz$$

If we assume that the recombination is only a small perturbation to the fast carriers' density (n_e):

(80) $$\frac{1}{q} \frac{\partial}{\partial t} Q_h(t) = \mu_h \frac{V}{d} n_h(d,t) - B n_e \int_0^d n_h(z,t) dz$$

(81) $$\frac{\partial}{\partial t} Q_h(t) = -B n_e \left[Q_h(t) - \mu_h \frac{qV}{d} \frac{n_h(d,t)}{B n_e} \right]$$

If we let $Q_h(t=0^+)=Q_{h0}$ where $Q_h(t=0^+)$ is the total hole charge at the end of the electrons transient:

(82) $$Q_h(t)=\mu_h\frac{qV}{d}\frac{n_h(d,t)}{Bn_e}+\left(Q_{h0}-\mu_h\frac{qV}{d}\frac{n_h(d,t)}{Bn_e}\right)e^{-Bn_e t}$$

From equation (82) we find that the time constant τ has the form $\frac{1}{\tau}=Bn_e$ and assuming the recombination to be Langevin: $\frac{1}{\tau}=\frac{q}{\varepsilon\varepsilon_0}(\mu_e+\mu_h)n_e\cong\frac{q}{\varepsilon\varepsilon_0}\mu_e n_e$. Namely, by extracting μ_e from the fast response and τ from the slow response we can deduce the fast carrier density:

(83) $$n_e\cong\frac{\varepsilon\varepsilon_0}{q\tau\mu_e}.$$

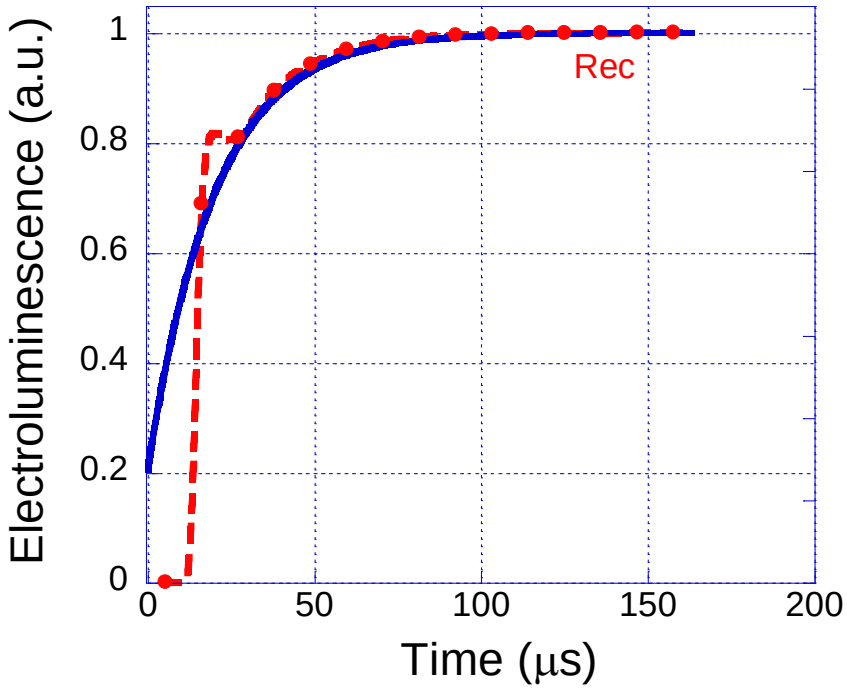

Figure 24. The full response including the slow component of the light turn on. The solid (red) curve is a fit to equation (82).

For example, in Figure 24 the full response of the same simulation presented in Figure 18 (dashed line, round symbols). The full blue line is a fit to equation (82) which results in $\tau=2\times10^{-5}$sec. From this we can deduce the fast carrier density in the region close to the

contact injecting the slow carriers: $n_{fast} \cong \frac{3*8.85\cdot10^{-14}}{1.6\cdot10^{-19}*2\cdot10^{-5}*1.33\cdot10^{-6}} \cong 6\cdot10^{16} cm^{-3}$

which is very similar to the density found in the simulation ($6.5x10^{16}cm^{-3}$) and presented in Figure 18.

As the process of filling the device with slow carriers is recombination limited it is obvious that $\tau_{tr\_slow} > \tau$ or that $\mu_{slow}<1x10^{-6}cm^2/Vs$.

(84) $$Q_{h0} = \theta\left[\mu_h \frac{V}{d}\frac{n_h(d,t)}{Bn_e}\right]$$

(85) $$\begin{cases} L_h = \dfrac{Q_h(\tau_{tr\_fast})}{qn_h(d,t)} = \mu_h \dfrac{V}{d}\tau\left[1+(\theta-1)e^{-\frac{\tau_{tr\_fast}}{\tau}}\right] \\ \dfrac{L_h}{d} = \dfrac{\mu_h}{\mu_e} \end{cases}$$

(86) $$\mu_e = \frac{d^2}{V\tau}\left[1+(\theta-1)e^{-\frac{\tau_{tr\_fast}}{\tau}}\right]^{-1}$$

And using this last expression we find $\mu_e=1.5x10^{-6}cm^2/Vs$.

Regarding the slow carrier mobility we can only deduce an upper limit for it. Examining Figure 24 we note that the exponential function is not disturbed up to ~100μs so we can state that τ_{tr_slow} is larger than that or that $\mu_h<2x10^{-7}cm^2/Vs$ (in the simulation code we used $\mu_h=5x10^{-8}cm^2/Vs$).

(2) Low efficiency case

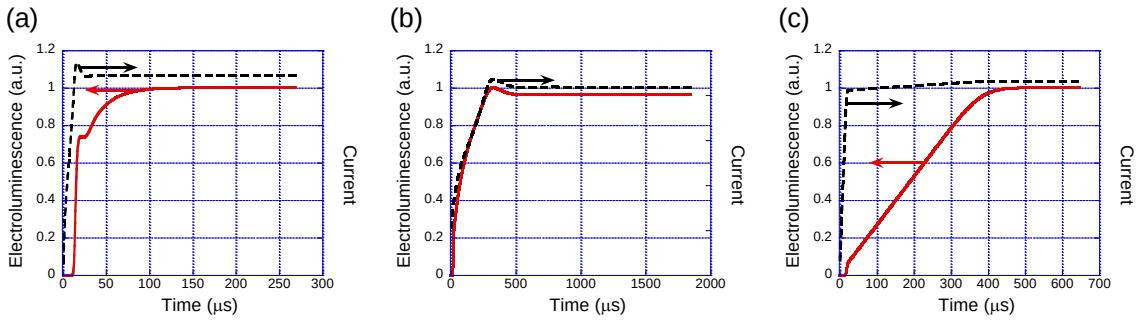

Figure 25. (a) slow carrier are contact limited ($n_e(0)$~$10^{18}cm^{-3}$; $n_h(d)=10^{14}cm^{-3}$). (b) fast carriers are contact limited and slow carriers are bulk limited ($n_e(0)$~$10^{14}cm^{-3}$; $n_h(d)=10^{18}cm^{-3}$). (c) both carriers are contact limited ($n_e(0)$~$10^{14}cm^{-3}$; $n_h(d)=10^{14}cm^{-3}$). Dashed line is the current and the full line is the recombination rate (~EL).

In Figure 25 we see three cases:
(a) The slow carriers are contact limited (almost no difference compared to Figure 24).
(b) The fast carriers are contact limited and the slow carriers are bulk limited. In this case the long time EL reflects the evolution of the density of slow carriers and is very similar to the current which is SCL.
(c) Both carrier are contact limited and the long time EL response again reflects the evolution of the density of slow carriers. However, in this case the flow into the device is not limited by recombination or space-charge and hence it follows conditions similar to those describes in section V.C “Optical step function excitation”.

VI.B. Frequency Domain

For a single carrier injection we can start by writing the transport equations neglecting diffusion and follow [14]:

$$\begin{aligned} V &= V_0 + V_1 \\ E &= E_0(z) + E_1(z,t) \\ n_e &= n_{e0}(z) + n_{e1}(z,t) \\ J_e &= J_{e0} + J_{e1}(t) \end{aligned} \quad (87)$$

Here subscript "0" denotes steady state and "1" is the small signal quantity.

$$-J_{e1} = \varepsilon\varepsilon_0 \frac{d}{dt} E_1(z,t) + q\mu_e n_{e0}(z) E_1(z,t) + q\mu_e n_{e1}(z,t) E_0(z) \quad (88)$$

$$-J_{e1} = \varepsilon\varepsilon_0 \frac{d}{dt} E_1(z,t) + q\mu_e n_{e0}(z) E_1(z,t) - \varepsilon\varepsilon_0 \mu_e E_0(z) \frac{d}{dz} E_1(z,t) \quad (89)$$

Laplace transform:

$$-j_{e1}(s) = \varepsilon\varepsilon_0 \left[s e_1(z,s) - E_1(z,0) \right] + q\mu_e n_{e0}(z) e_1(z,s) - \varepsilon\varepsilon_0 \mu_e E_0(z) \frac{d}{dz} e_1(z,s) \quad (90)$$

Where the small letters denote the transformed variable.

$$\frac{d}{dz} e_1(z,s) - \frac{q\mu_e n_{e0}(z) + \varepsilon\varepsilon_0 s}{\varepsilon\varepsilon_0 \mu_e E_0(z)} e_1(z,s) = \frac{+ j_{e1}(s) - \varepsilon\varepsilon_0 E_1(z,0)}{\varepsilon\varepsilon_0 \mu_e E_0(z)} \quad (91)$$

Equation (91) needs to be solved using the appropriate boundary conditions. The result is then integrated to yield a relation between the voltage (V_1) and the current (j_{e1}):

$$-v_1(s) = \int_0^d e_1(z,s) dz$$

from which the admittance (j_{e1}/V_1) frequency response can be derived (For a frequency independent excitation the time dependence of the voltage excitation has to be a delta function). At t=0 the charges have not yet moved in the device and hence the small signal electric field $E_1(z,0) = const$ and for a delta function excitation: $E_1(z,0) = 0$.

SCL conditions:

In reference [14] the problem is solved for the case of space charge limited current where one uses the common approximations of:

(92) $E_0(z) = -\sqrt{\frac{2J_{0e}z}{\varepsilon\varepsilon_0\mu_e}}$, $n_{e0}(z) = \frac{1}{q}\sqrt{\frac{\varepsilon\varepsilon_0 J_{0e}}{2\mu_e z}}$, $J_{0e} = \frac{9}{8}\varepsilon\varepsilon_0\mu_e\frac{V_0^2}{d^3}$;

As implied above, for SCL current the electric field at the injecting contact is zero and hence:

(93) $e_1(0,s) = 0$

Using above equations one can derive (see Appendix 1 – Frequency response SCL) the following:

(94) $Y \triangleq \frac{j_1}{V_1} \triangleq G + jB = \frac{2(\varepsilon\varepsilon_0)^2}{\mu j_0 \tau_{tr}^3}\frac{(i\omega\tau_{tr})^3}{(i\omega)^2\tau_{tr}^2 - 2i\omega\tau_{tr} + 2 - 2e^{-j\omega\tau_{tr}}}$

Contact limited (non metallic contact):

In this case the charge density at the contact is fixed by the contact work-function. As the contact is not metallic there is no image force effect and the contact barrier is independent of voltage.

For contact limited: $E_0(z) \approx E_0 = -\frac{V_0}{d}$, $n_{e0}(z) = n_{e0}(0) - az$, $a = \frac{n_{e0}^2(0)dq}{V_0\varepsilon\varepsilon_0}$;

at t=0 $E_1(z,0) = 0$ and as the charge density at the injecting contact is fixed $\frac{d}{dz}e_1(0,s) = 0$

Solving for these conditions: (to be completed, Nir)

Contact limited (metallic contact): (to be completed, Nir)

SCL conditions (single carrier injection)

In all the previous sections we started with simulations results to promote some level of intuitive understanding. For consistency we do the same here although it seems that in the current case the contribution of the numerical results to the intuitive understanding is very small. In this simulation the contact barriers are set at 0.15eV for electrons and 0.5eV for holes making the electron injection not limited by the contact and the hole injection is negligible. The electrons are 10 times faster than the holes ($\mu_h=0.1\mu_e$; $\mu_e=10^{-6}cm^2/Vs$), the device length is d=100nm, and the DC applied voltage is (V-Vbi)=5V. In the simulation we first apply a step voltage of 5V and allow the device to reach steady state (see Figure 26a). At t=170μs we add to the voltage a small step which is 10^{-3} of the large signal applied to turn the device on. Figure 26b shows a zoom on the small signal current response to the 5mV increase in voltage.

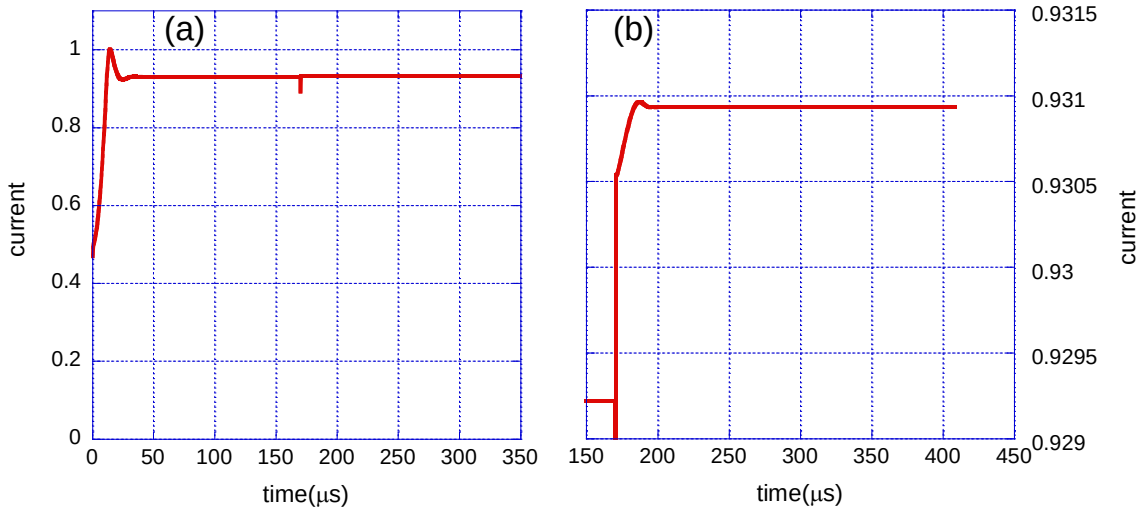

Figure 26. (a) Current response to a step voltage excitation of 0 to 5V at t=0 and 5v to 5.005V at t=170μs. (b) zoom on the response to the small (5mV) step at t=170μs.

After verifying that the response is linear with the applied small-step height we can calculate the impulse response by differentiating (d/dt) the step response. This procedure is shown in Figure 27.

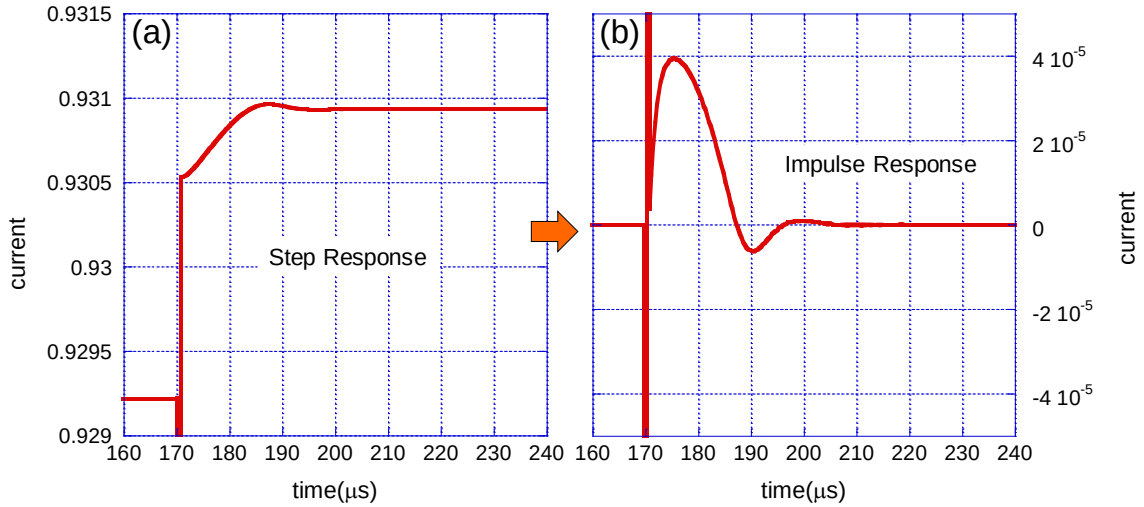

Figure 27. (a) The small signal step response shown in Figure 26b (b) The impulse response derived by applying d/dt to the data in (a).

Finally, the frequency response is calculated by Fourier transforming the impulse response. Figure 28 illustrates this procedure and Figure 28b shows the real and imaginary parts of the response which are proportional to the conductance and susceptance, respectively. The angle shown at the top of Figure 28b uses $w = 2\pi f$ and $\tau_{tr} = \dfrac{d^2}{\mu_e V}$.

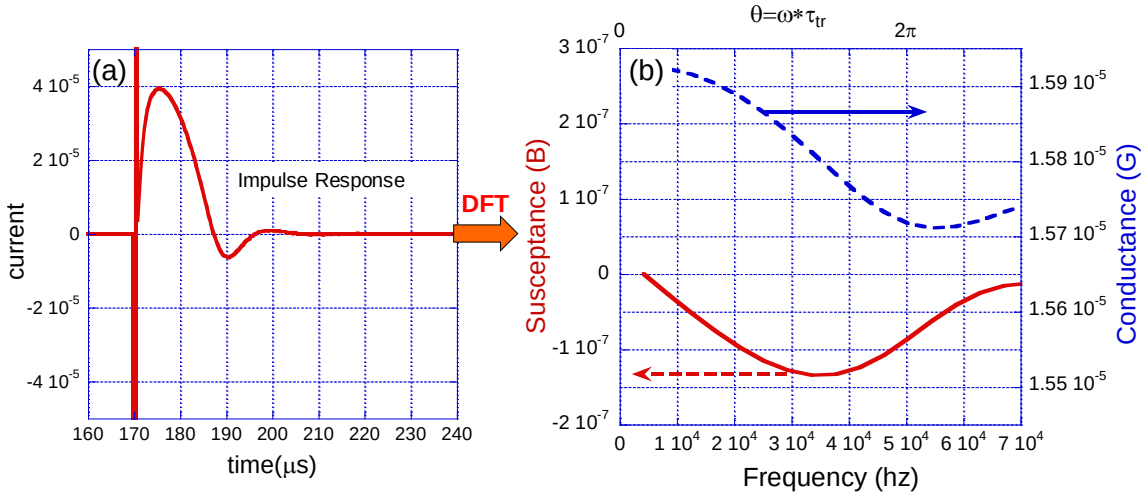

Figure 28. (a) The impulse response shown in Figure 27b. (b) The frequency response calculated by Fourier transforming the impulse response. The real and imaginary parts are proportional to the conductance and susceptance, respectively.

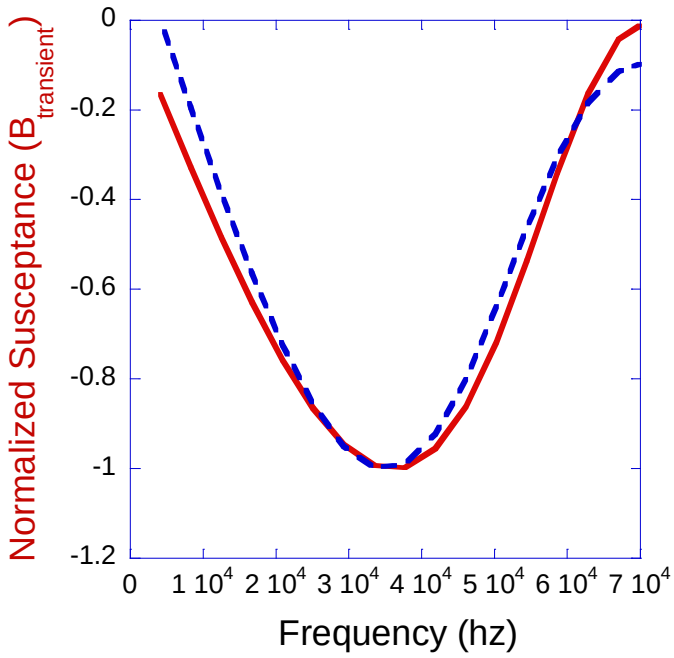

Figure 29. The transient related susceptance as calculated using equation (94) [solid line] and the one deduced from the numerical simulations [dashed line].

VII. Appendix 1 – Frequency response SCL

(95) $$\frac{d}{dz}e_1(z,s)-\frac{q\mu_e n_{e0}(z)+\varepsilon\varepsilon_0 s}{\varepsilon\varepsilon_0\mu_e E_0(z)}e_1(z,s)=\frac{+j_{e1}(s)-\varepsilon\varepsilon_0 E_1(z,0)}{\varepsilon\varepsilon_0\mu_e E_0(z)}$$

Equation (91) needs to be solved using the appropriate boundary conditions. The result is then integrated to yield a relation between the voltage (V_1) and the current (j_{e1}):

$$-V_1(s)=\int_0^d e_1(z,s)dz$$

from which the admittance (j_{e1}/V_1) frequency response can be derived (For a frequency independent excitation the time dependence of the voltage excitation has to be a delta function). The initial condition for the small signal electric field at t=0, before applying the small signal perturbation, is $E_1(z,0)=0$.

In reference [14] the problem is solved for the case of space charge limited current where one uses the common approximations of:

(96) $$E_0(z)=-\sqrt{\frac{2J_{0e}z}{\varepsilon\varepsilon_0\mu_e}},\ n_{e0}(z)=\frac{1}{q}\sqrt{\frac{\varepsilon\varepsilon_0 J_{0e}}{2\mu_e z}},\ J_{0e}=\frac{9}{8}\varepsilon\varepsilon_0\mu_e\frac{V_0^{\,2}}{d^3};$$

As implied above, for SCL current the electric field at the injecting contact is zero and hence:

(97) $$e_1(0,s)=0$$

Solving the differential equation

$$\theta=\exp\left[-\int\frac{q\mu_e n_{e0}(z)+\varepsilon\varepsilon_0 s}{\varepsilon\varepsilon_0\mu_e E_0(z)}dz\right]=\exp\left[\int\frac{\mu_e\sqrt{\frac{\varepsilon\varepsilon_0 J_{0e}}{2\mu_e z}}+\varepsilon\varepsilon_0 s}{\varepsilon\varepsilon_0\mu_e\sqrt{\frac{2J_{0e}z}{\varepsilon\varepsilon_0\mu_e}}}dz\right]=$$

(98) $$\theta=\exp\left[\int\left[\frac{1}{2z}+\frac{\varepsilon\varepsilon_0 s}{\sqrt{2\varepsilon\varepsilon_0\mu_e J_{0e}z}}\right]dz\right]=\exp\left[\left[\ln(z^{\frac{1}{2}})+\frac{2\varepsilon\varepsilon_0 s}{\sqrt{2\varepsilon\varepsilon_0\mu_e J_{0e}}}z^{\frac{1}{2}}\right]\right]=$$

$$\theta=z^{\frac{1}{2}}\exp\left[\frac{2\varepsilon\varepsilon_0 s}{\sqrt{2\varepsilon\varepsilon_0\mu_e J_{0e}}}z^{\frac{1}{2}}\right]$$

$$\varsigma = \int_0^{z'} \theta\left(\frac{+j_{e1}(s)}{\varepsilon\varepsilon_0\mu_e E_0(z)}\right)dz = \int_0^{z'} \theta\left(-\frac{+j_{e1}(s)}{\sqrt{2\varepsilon\varepsilon_0\mu_e J_{0e} z}}\right)dz$$

(99)

$$\varsigma = -\frac{+j_{e1}(s)}{\sqrt{2\varepsilon\varepsilon_0\mu_e J_{0e}}}\int_0^{z'} \exp\left[\frac{2\varepsilon\varepsilon_0 s}{\sqrt{2\varepsilon\varepsilon_0\mu_e J_{0e}}} z^{\frac{1}{2}}\right]dz =$$

$$\int e^{a\sqrt{z}}\, dz = 2\, e^{a\sqrt{z}}\left(\frac{\sqrt{z}}{a} - \frac{1}{a^2}\right)$$

$$\varsigma = -\frac{+j_{e1}(s)}{\sqrt{2\varepsilon\varepsilon_0\mu_e J_{0e}}} 2\exp\left[\frac{2\varepsilon\varepsilon_0 s}{\sqrt{2\varepsilon\varepsilon_0\mu_e J_{0e}}} z^{\frac{1}{2}}\right]\left(\frac{\sqrt{2\varepsilon\varepsilon_0\mu_e J_{0e}}}{2\varepsilon\varepsilon_0 s} z^{\frac{1}{2}} - \frac{\mu_e J_{0e}}{2\varepsilon\varepsilon_0 s^2}\right)$$

$$e_1(z,s) = \frac{1}{z^{\frac{1}{2}}\exp\left[\frac{2\varepsilon\varepsilon_0 s}{\sqrt{2\varepsilon\varepsilon_0\mu_e J_{0e}}} z^{\frac{1}{2}}\right]}\left\{c - \frac{+j_{e1}(s)}{\sqrt{2\varepsilon\varepsilon_0\mu_e J_{0e}}} 2\exp\left[\frac{2\varepsilon\varepsilon_0 s}{\sqrt{2\varepsilon\varepsilon_0\mu_e J_{0e}}} z^{\frac{1}{2}}\right]\left(\frac{\sqrt{2\varepsilon\varepsilon_0\mu_e J_{0e}}}{2\varepsilon\varepsilon_0 s} z^{\frac{1}{2}} - \frac{\mu_e J_{0e}}{2\varepsilon\varepsilon_0 s^2}\right)\right\}$$

and as the electric field at the injecting contact is fixed at zero $e_1(0,s) = 0$

$$c = -\mu_e J_{0e}\frac{+j_{e1}(s)}{\varepsilon\varepsilon_0\sqrt{2\varepsilon\varepsilon_0\mu_e J_{0e}}}\frac{1}{s^2}$$

$$e_1(z,s) = -\frac{+j_{e1}(s)}{\varepsilon\varepsilon_0 s}\left\{\mu_e J_{0e}\frac{1}{\sqrt{2\varepsilon\varepsilon_0\mu_e J_{0e}}}\frac{1}{\sqrt{zs}}\exp\left[-\frac{2\varepsilon\varepsilon_0 s}{\sqrt{2\varepsilon\varepsilon_0\mu_e J_{0e}}} z^{\frac{1}{2}}\right] + 1 - \frac{\sqrt{\mu_e J_{0e}}}{\sqrt{2\varepsilon\varepsilon_0}\sqrt{zs}}\right\}$$

Inserting: $J_{0e} = \frac{9}{8}\varepsilon\varepsilon_0\mu_e\frac{V_0^2}{d^3}$

$$e_1(z,s) = -\frac{+j_{e1}(s)}{\varepsilon\varepsilon_0 s}\left\{\frac{3}{4}\frac{\mu_e V_0}{d^2}\frac{1}{\sqrt{\frac{z}{d}s}}\exp\left[-\frac{s}{\frac{3}{4}\frac{\mu_e V_0}{d^2}}\sqrt{\frac{z}{d}}\right] + 1 - \frac{\frac{3}{4}\frac{\mu_e V_0}{d^2}}{\sqrt{\frac{z}{d}s}}\right\}$$

$$T_0 = \sqrt{\frac{2\varepsilon\varepsilon_0 d}{\mu_e J_{0e}}} = \sqrt{\frac{16d^4}{\mu_e 9\mu_e V_0^2}} = \frac{4}{3}\frac{d^2}{\mu_e V_0} = \frac{4}{3}\tau_{tr}$$

Introducing a normalized distance $\psi = \frac{z}{d}$

$$e_1(\psi,s) = -\frac{+j_{e1}(s)}{\varepsilon\varepsilon_0 s}\left\{1 - \frac{1}{\sqrt{\psi}T_0 s} + \frac{1}{\sqrt{\psi}T_0 s}\exp\left[-T_0 s\sqrt{\psi}\right]\right\}$$

$$V_1(s) = \frac{+j_{e1}(s)}{\varepsilon\varepsilon_0 s}d\left\{1 + \int_0^1\left\{\frac{1}{\sqrt{\psi}T_0 s}\exp\left[-T_0 s\sqrt{\psi}\right]\right\}d\psi - \int_0^1\left\{\frac{1}{\sqrt{\psi}T_0 s}\right\}d\psi\right\}$$

$$\int_0^1\left\{\frac{1}{\sqrt{\psi}T_0 s}\exp\left[-T_0 s\sqrt{\psi}\right]\right\}d\psi = -\frac{2}{(T_0 s)^2}\exp\left[-T_0 s\sqrt{\psi}\right]\Big|_0^1 = -\frac{2}{(T_0 s)^2}\exp\left[-T_0 s\right] + \frac{2}{(T_0 s)^2} = \frac{2}{(T_0 s)^2}\left(1-\exp\left[-T_0 s\right]\right)$$

$$\int_0^1\left\{\frac{1}{T_0 s\sqrt{\psi}}\right\}d\psi = \frac{2}{T_0 s}\sqrt{\psi}\Big|_0^1 = \frac{2}{T_0 s}$$

$$V_1(s) = \frac{+j_{e1}(s)}{\varepsilon\varepsilon_0 s}d\left\{1 + \frac{2}{(T_0 s)^2}\left(1-\exp\left[-T_0 s\right]\right) - \frac{2}{T_0 s}\right\} = \frac{+j_{e1}(s)}{\varepsilon\varepsilon_0 s}d\,\frac{(T_0 s)^2 + 2 - 2\exp\left[-T_0 s\right] - 2T_0 s}{(T_0 s)^2}$$

$$\frac{j_{e1}(s)}{V_1(s)} = \frac{\varepsilon\varepsilon_0}{T_0 d}\,\frac{(T_0 s)^3}{(T_0 s)^2 + 2 - 2\exp\left[-T_0 s\right] - 2T_0 s}$$

Alternative derivation:

The derivation here follows the one published by Shao et. al. [15] which derived the frequency dependent impedance $Y \triangleq \frac{j_1}{V_1} \triangleq G + jB$ where j_1 and V_1 are the small signal frequency dependent current and voltage.

We start by writing equation (7) for single carrier:

$$-j(z,t) = \varepsilon\varepsilon_0\frac{d}{dt}E(z,t) + j_e(z,t) = \varepsilon\varepsilon_0\frac{d}{dt}E(z,t) + q\mu_e n_e(z,t)E(z,t) + qD_e\frac{d}{dz}n_e(z,t)$$

Neglecting diffusion:

$$(100)\quad -j(z,t) = \varepsilon\varepsilon_0\frac{d}{dt}E(z,t) + j_e(z,t) = \varepsilon\varepsilon_0\frac{d}{dt}E(z,t) + q\mu_e n_e(z,t)E(z,t)$$

To this we add the Poisson equation:

$$\frac{d}{dz}E = -\frac{q}{\varepsilon\varepsilon_0}n_e(z)$$

To solve the response to a small signal we start by following an electron moving from one side of sample to the other at a velocity that is dictated by the electric field. We will also assume that the electron is leaving at $t=t_c$ and that it leaves the electrode with a zero velocity (under SCL condition the electric field is zero at the contact). This electron is moving at a velocity $v = \frac{dz}{dt}$ and is experiencing an electric field that is changing according to:

(101) $\frac{dE}{dt}=\frac{\partial E}{\partial z}\frac{dz}{dt}+\frac{\partial E}{\partial t}=\frac{q}{\varepsilon\varepsilon_0}n_e(z)\cdot\mu_e E(z,t)+\frac{\partial E}{\partial t}$

Using equations *(101)* and (100) we find

(102) $-j(z,t)=\frac{\varepsilon\varepsilon_0}{\mu_e}\frac{d}{dt}\left[\mu_e E_e(z,t)\right]$

or

(103) $j(z,t)=\frac{\varepsilon\varepsilon_0}{\mu_e}\frac{d}{dt}v=\frac{\varepsilon\varepsilon_0}{\mu_e}\frac{d}{dt}\frac{dz}{dt}$

A common method for solving small signal frequency response is to let all variables take the form of $a=a_0+a_1\cdot e^{i\omega t}$ where a_1 is the small signal of the variable *a*. using this approach we write the current associated with the moving electron as:

(104) $j=j_0+j_1\cdot e^{i\omega t}$

Inserting *(104)* into *(103)* and integrating with respect to t:

$$v=\frac{\mu_e}{\varepsilon\varepsilon_0}\left(j_0 t+\frac{j_1\cdot e^{i\omega t}}{i\omega}\right)+const$$

Using the assumption that the charge leaves the contact at t=t_c with a velocity of *v*=0:

(105) $v=\frac{\mu_e}{\varepsilon\varepsilon_0}\left(j_0\left(t-t_c\right)+\frac{j_1\cdot\left(e^{i\omega t}-e^{i\omega t_c}\right)}{i\omega}\right)$

By integrating *(105)* and knowing that at t=t_c z=0 we deduce the distance traveled by the electron as:

(106) $z=\frac{\mu}{\varepsilon}\left(\frac{j_0\left(t-t_c\right)^2}{2}-\frac{j_1\left(t-t_c\right)\cdot e^{i\omega t_c}}{i\omega}-\frac{j_1\cdot\left(e^{i\omega t}-e^{i\omega t_c}\right)}{\omega^2}\right)$

So, if we consider a single carrier exiting the contact at t=t_c we can use equation *(105)* and *(106)* to know where it would be or what would be its velocity at time t (t - t_c). However, as these equations show, the result is NOT independent of the time at which the charge started its travel (t_c). This could be understood if we realize that depending on where on the modulation cycle the charge starts its travel it experiences a slightly different voltage or field as it crosses the sample. To find a solution that is independent of t_c (frequency response is by definition time independent) we represent the time it takes to reach point z as a small signal response:

(107) $t-t_c=T_0+T_1\cdot e^{i\omega t}$

Here T_0 is the mean time to reach z and T_1 is the change in the time it takes to reach that point under modulation conditions. Namely, we replace the unknown t_c with T_1 and our goal in the following would be to find an expression for T_1. Inserting *(107)* into (105) and neglecting higher order terms:

$$(108)\; v \approx \frac{\mu}{\varepsilon\varepsilon_0}\left(j_0\left(T_0 + T_1\cdot e^{i\omega t}\right) + \frac{j_1\cdot\left(e^{i\omega t} - e^{i\omega\left(t-T_0-T_1 e^{i\omega t}\right)}\right)}{i\omega}\right)$$

And similarly with equation *(106)*

$$(109)\; z \approx \frac{\mu}{\varepsilon\varepsilon_0}\left(\frac{j_0\left(T_0 + T_1 e^{j\omega t}\right)^2}{2} - \frac{j_1\left(T_0 + T_1 e^{j\omega t}\right)\cdot e^{i\omega(t-T_0)}}{j\omega} - \frac{J_1\cdot\left(e^{i\omega t} - e^{i\omega(t-T_0)}\right)}{\omega^2}\right)$$

Arranging and neglecting higher frequencies (or higher orders):

$$(110)\; z = z_0 + z_1 e^{i\omega t} \approx \frac{\mu}{\varepsilon\varepsilon_0}\left(\frac{j_0\left(T_0{}^2 + 2T_0T_1 e^{i\omega t}\right)}{2} - \frac{j_1T_0\cdot e^{i\omega(t-T_0)}}{i\omega} - \frac{J_1\cdot e^{i\omega t}\left(1-e^{-i\omega T_0}\right)}{\omega^2}\right)$$

From this we can deduce the mean and time varying position as:

$$(111)\; z_0 = \frac{j_0\mu}{2\varepsilon\varepsilon_0}T_0{}^2$$

$$(112)\; z_1 e^{i\omega t} = \frac{\mu}{\varepsilon\varepsilon_0}\left(j_0T_0T_1 e^{i\omega t} - \frac{j_1T_0\cdot e^{i\omega(t-T_0)}}{i\omega} - \frac{J_1\cdot e^{i\omega t}\left(1-e^{-i\omega T_0}\right)}{\omega^2}\right)$$

To find T_1 we recall that we defined $t - t_c = T_0 + T_1\cdot e^{i\omega t}$ as the time needed to reach a time-independent position z (or z_0 in the current notation). Namely, according to our definition $z_1 \equiv 0$ and from *(112)* T_1 can be expressed as:

$$(113)\; T_1 = \frac{j_1\cdot e^{-i\omega T_0}}{j_0 i\omega} + \frac{j_1\left(1-e^{-i\omega T_0}\right)}{j_0T_0\omega^2}$$

Now we are set to find the frequency response that is independent of time (t_c). Inserting *(113)* into (108):

$$v \approx \frac{\mu}{\varepsilon\varepsilon_0}\left(j_0T_0 + \frac{j_1\cdot e^{i\omega(t-T_0)}}{i\omega} + \frac{j_1e^{i\omega t}\left(1-e^{-i\omega T_0}\right)}{T_0\omega^2} + \frac{j_1\cdot\left(e^{i\omega t} - e^{i\omega(t-T_0)}\right)}{i\omega}\right)$$

And rearranging:

$$(114)\; v \approx \frac{\mu}{\varepsilon\varepsilon_0}\left(j_0T_0 + \frac{j_1e^{i\omega t}\left(1-e^{-i\omega T_0}\right)}{T_0\omega^2} + \frac{j_1\cdot e^{i\omega t}}{i\omega}\right)$$

$$V = -\int_0^d E\cdot dz = \frac{1}{\mu}\int_0^d v\cdot dz$$

Using *(111)* $dz = \frac{j_0\mu}{\varepsilon\varepsilon_0}T_0 dT_0$

$$V_0 = \frac{1}{\varepsilon\varepsilon_0}\int_0^{\tau_{tr}} v_0 j_0 T_0 dT_0 = \frac{\mu}{(\varepsilon\varepsilon_0)^2} j_0^{\,2}\int_0^{\tau_{tr}} T_0^{\,2} dT_0 = \frac{\mu}{3(\varepsilon\varepsilon_0)^2} j_0^{\,2}\tau_{tr}^{\,3}$$

$$V_1 = \frac{1}{\mu}\int_0^{d} v_1 \cdot dz = \frac{1}{\mu}\int_0^{\tau_{tr}} \frac{\mu}{\varepsilon\varepsilon_0}\left(\frac{j_1\left(1-e^{-i\omega T_0}\right)}{T_0\omega^2} + \frac{j_1}{i\omega}\right)\cdot\frac{j_0\mu}{\varepsilon\varepsilon_0} T_0 dT_0$$

$$V_1 = \frac{j_1 j_0 \mu}{(\varepsilon\varepsilon_0)^2}\int_0^{\tau_{tr}}\left(\frac{\left(1-e^{-i\omega T_0}\right)}{\omega^2} + \frac{T_0}{i\omega}\right)\cdot dT_0 = \frac{j_1 j_0 \mu}{(\varepsilon\varepsilon_0)^2}\left(-\frac{\tau_{tr}}{(i\omega)^2} - \frac{e^{-i\omega\tau_{tr}}-1}{(i\omega)^3} + \frac{\tau_{tr}^{\,2}}{2i\omega}\right)$$

And finally:

$$(115)\; Y \triangleq \frac{j_1}{V_1} \triangleq G + jB = \frac{2(\varepsilon\varepsilon_0)^2}{\mu j_0}\frac{(i\omega)^3}{(i\omega)^2\tau_{tr}^{\,2} - 2i\omega\tau_{tr} + 2 - 2e^{-j\omega\tau_{tr}}}$$

$$G \triangleq \mathrm{Re}\left\{\frac{j_1}{V_1}\right\} = \frac{2(\varepsilon\varepsilon_0)^2}{\mu j_0}\mathrm{Re}\left\{\frac{(i\omega)^3}{(i\omega)^2\tau_{tr}^{\,2} - 2i\omega\tau_{tr} + 2 - 2e^{-i\omega\tau_{tr}}}\right\} =$$

$$= \frac{2(\varepsilon\varepsilon_0)^2}{\mu j_0}\mathrm{Re}\left\{\frac{-i\omega^3}{2-\omega^2\tau_{tr}^{\,2} - 2\cos(\omega\tau_{tr}) + 2i\sin(\omega\tau_{tr}) - 2i\omega\tau_{tr}}\right\} =$$

$$= \frac{2(\varepsilon\varepsilon_0)^2}{\mu j_0}\mathrm{Re}\left\{\frac{-i\omega^3\left[2-\omega^2\tau_{tr}^{\,2} - 2\cos(\omega\tau_{tr}) - 2i\sin(\omega\tau_{tr}) + 2i\omega\tau_{tr}\right]}{\left[2-\omega^2\tau_{tr}^{\,2} - 2\cos(\omega\tau_{tr})\right]^2 + \left[2\sin(\omega\tau_{tr}) - 2\omega\tau_{tr}\right]^2}\right\} =$$

$$= \frac{(\varepsilon\varepsilon_0)^2}{\mu j_0\tau_{tr}^{\,3}}\frac{(\omega\tau_{tr})^3\left[\omega\tau_{tr} - \sin(\omega\tau_{tr})\right]}{\left[(\omega\tau_{tr})^2/2 + \cos(\omega\tau_{tr}) - 1\right]^2 + \left[\sin(\omega\tau_{tr}) - \omega\tau_{tr}\right]^2}$$

$$\frac{\partial V_0}{\partial j_0} = \frac{2\mu}{3(\varepsilon\varepsilon_0)^2} j_0\tau_{tr}^{\,3}$$

By defining $g \triangleq \frac{\partial j_0}{\partial V_0} = \frac{3(\varepsilon\varepsilon_0)^2}{2\mu j_0\tau_{tr}^{\,3}}$; $\theta \triangleq \omega\tau_{tr}$ we find the expression for the conductance and susceptance:

$$G \triangleq \mathrm{Re}\left\{\frac{j_1}{V_1}\right\} = \frac{2g\theta^3}{3}\frac{\left[\theta - \sin(\theta)\right]}{\left[(\theta)^2/2 + \cos(\theta) - 1\right]^2 + \left[\sin(\theta) - \theta\right]^2}$$

$$B(\theta) \triangleq \mathrm{Im}\left\{\frac{j_1}{V_1}\right\} = \frac{2g\theta^3}{3} \cdot \frac{\theta^2/2 + \cos\theta - 1}{(\theta - \sin\theta)^2 + \left(\theta^2/2 + \cos\theta - 1\right)^2}$$

The high frequency limit susceptance of the device is due to its geometric capacitance:

$$B(\theta)\big|_{\theta\to\infty} \triangleq \mathrm{Im}\left\{\frac{j_1}{V_1}\right\} = \frac{4g\theta}{3}$$

To find the contribution due to the transport we subtract it from the overall susceptance:

$$(116)\ B(\theta)_{transient} \triangleq B(\theta) - B(\theta)\big|_{\theta\to\infty} = \frac{2g}{3} \cdot \left\{ \theta^3 \frac{\theta^2/2 + \cos\theta - 1}{(\theta - \sin\theta)^2 + \left(\theta^2/2 + \cos\theta - 1\right)^2} - 2\theta \right\}$$

References

[1] M. A. Lampert and P. Mark, *Current injection in solids*. New York: Academic Press, 1970.

[2] K. C. Kao and W. Hwang, *Electrical transport in solids* vol. 14. New York: Pergamon press, 1981.

[3] M. Van der Auweraer, F. C. Deschryver, P. M. Borsenberger, and H. Bassler, "Disorder in Charge-Transport in Doped Polymers," *Advanced Materials,* vol. 6, pp. 199-213, 1994.

[4] E. M. Horsche, D. Haarer, and H. Scher, "Transition from dispersive to nondispersive transport: Photoconduction of polyvinylcarbazole," *Phys. Rev. B,* vol. 35, pp. 1273-1280, 1987.

[5] H. Scher and E. M. Montroll, "Anomalous transit-time dispersion in amorphous solids," *Phys. Rev. B,* vol. 12, pp. 2455–2477, 1975.

[6] H. Scher, M. F. Shlesinger, and J. T. Bendler, "TIME-SCALE INVARIANCE IN TRANSPORT AND RELAXATION," *Physics Today,* vol. 44, pp. 26-34, 1991.

[7] G. Juska, K. Arlauskas, M. ViliÅ«nas, and J. KoÄ • ka, "Extraction Current Transients: New Method of Study of Charge Transport in Microcrystalline Silicon," *Physical Review Letters,* vol. 84, p. 4946, 2000.

[8] G. Juska, K. Genevicius, K. Arlauskas, R. Osterbacka, and H. Stubb, "Charge transport at low electric fields in pi-conjugated polymers," *Phys. Rev. B,* vol. 65, pp. art. no.-233208, 2002.

[9] A. Pivrikas, N. S. Sariciftci, G. Juska, and R. Osterbacka, "A review of charge transport and recombination in polymer/fullerene organic solar cells," *Progress in Photovoltaics,* vol. 15, pp. 677-696, Dec 2007.

[10] D. J. Pinner, R. H. Friend, and N. Tessler, "Transient electroluminescence of polymer light emitting diodes using electrical pulses," *J. Appl. Phys.,* vol. 86, pp. 5116-5130, 1999.

[11] N. Rappaport, O. Solomesch, and N. Tessler, "The mobility spatial distribution function: Turn-on dynamics of polymer photocells," *Journal of Applied Physics,* vol. 99, p. 064507, Mar 2006.

[12] N. Rappaport, Y. Bar, O. Solomeshch, and N. Tessler, "Mobility spatial distribution function: Comparative method for conjugated polymers/molecules," *Applied Physics Letters,* vol. 89, p. 252117, Dec 2006.

[13] N. Rappaport, Y. Preezant, and N. Tessler, "Spatially dispersive transport: A mesoscopic phenomenon in disordered organic semiconductors," *Physical Review B,* vol. 76, p. 235323, Dec 2007.

[14] R. Baron, M. A. Nicolet, and V. Rodriguez, "Differential Step Response of Unipolar Space-Charge-Limited Current in Solids," *Journal of Applied Physics,* vol. 37, pp. 4156-4158, 1966.

[15] J. Shao and G. T. Wright, "Characteristics of the space charge limited dielectric diode at very high frequencies," *Solid-state electronics,* vol. 3, pp. 291-303, 1961.